

Finite Horizon Optimization: Framework and Applications ^{*}

Yushun Zhang¹², Dmitry Rybin¹², Zhi-Quan Luo^{12†}

¹The Chinese University of Hong Kong, Shenzhen, China

²Shenzhen Research Institute of Big Data

{yushunzhang,dmitryrybin}@link.cuhk.edu.cn, luozq@cuhk.edu.cn

Abstract

In modern engineering scenarios, there is often a strict upper bound on the number of algorithm iterations that can be performed within a given time limit. This raises the question of optimal algorithmic configuration for a fixed and finite iteration budget. In this work, we introduce the framework of *finite horizon optimization*, which focuses on optimizing the algorithm performance under a strict iteration budget T . We apply this framework to linear programming (LP) and propose Finite Horizon stepsize rule for the primal-dual method. The main challenge in the stepsize design is controlling the singular values of T cumulative product of non-symmetric matrices, which appears to be a highly nonconvex problem, and there are very few helpful tools. Fortunately, in the special case of the primal-dual method, we find that the optimal stepsize design problem admits hidden convexity, and we propose a convex semidefinite programming (SDP) reformulation. This SDP only involves matrix constraints of size 4×4 and can be solved efficiently in negligible time. Theoretical acceleration guarantee is also provided at the pre-fixed T -th iteration, but with no asymptotic guarantee. On more than 90 real-world LP instances, Finite Horizon stepsize rule reaches an average $3.9\times$ speed-up over the optimal constant stepsize, saving 75% wall-clock time. Our numerical results reveal substantial room for improvement when we abandon asymptotic guarantees, and instead focus on the performance under finite horizon. We highlight that the benefits are not merely theoretical - they translate directly into computational speed-up on real-world problems. ¹

1 Introduction

In the field of optimization, iterative algorithms are often equipped with tunable hyperparameters. For example, Gradient Descent (GD) has a hyperparameter called stepsize, which determines the magnitude of the adjustment made in each iteration [Cauchy et al., 1847]. These hyperparameters significantly affect the algorithm’s performance, influencing whether it diverges, converges, or how fast it converges. Theoretical analysis is crucial for guiding the proper selection of hyperparameters. The mainstream theoretical analysis guides the selection of hyperparameters through the following procedure. First, we fix the class of functions and fix the rule for selecting a category of hyperparameters (e.g., constant stepsize); second, we study the decay behavior of an optimality residue versus the iteration number T through asymptotic analysis, i.e., we aim to guarantee the good performance as $T \rightarrow \infty$. This methodology leads to many well-known results. For instance, the optimal constant stepsize for GD is $2/(\mu + L)$ for μ -strongly convex L -Lipschitz smooth functions [Nesterov et al., 2018]. Such theoretical insights have significantly deepened our understanding of iterative algorithms and have guided engineers for decades.

*: This is a preliminary report of an ongoing research.

†: Correspondence author.

¹Our code is available at <https://github.com/zyushun/Finite-Horizon-Stepsize-Rule>.

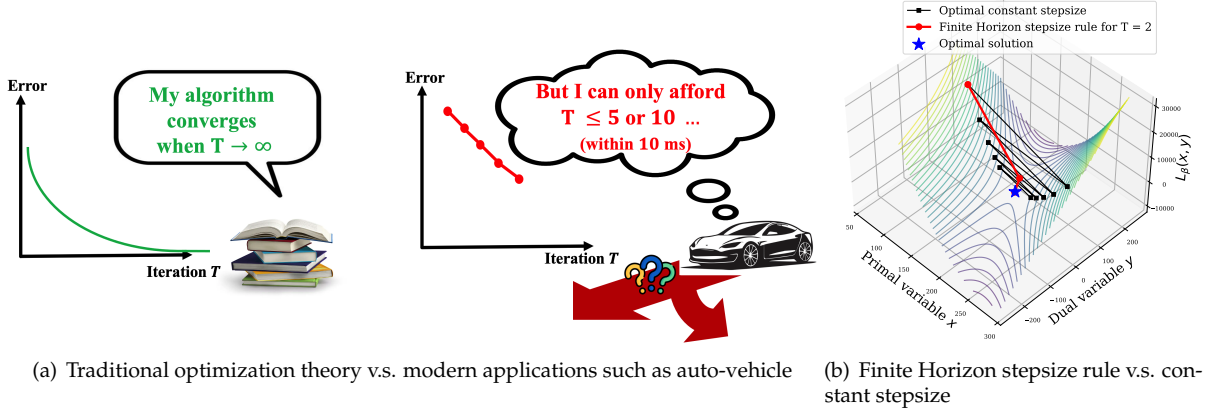


Figure 1: **(a)**: The growing mismatch between traditional optimization theory and modern applications such as auto-vehicle: classical theory focuses on $T \rightarrow \infty$, while many applications can only afford small T . **(b)**: The trajectories of Finite Horizon stepsize rule and the optimal constant stepsize on the augmented Lagrangian function of a simple linear programming (LP). The Finite Horizon stepsize rule for $T = 2$ reaches the optimal solution (the saddle) in 2 steps, while the optimal constant stepsize cannot.

Despite the long-standing and far-reaching impact of these theories, modern real-world applications are revealing new challenges. In particular, there is often a strict upper bound on the number of algorithm iterations that can be performed within a given time limit. For instance, in 5G or 6G wireless communication systems, iterative algorithms must operate at high throughput to ensure low-latency communications among users [Latva-Aho et al., 2019]. Typically, the iteration budget for the channel decoder algorithms is restricted to fewer than **5 iterations** (see Table 1 in [Sy, 2023]) or **15 iterations** (see Table IV in [Ferraz et al., 2021]). A comparable situation arises in modern power systems, where the average running time for iterative algorithms is **0.062 seconds** with **12 iterations** [Tang et al., 2017]. Similarly, for autonomous vehicles, real-time decision-making problems are often formulated as linear or quadratic programming, and the solvers must return solutions within **10 milliseconds (ms)** or **20 ms** [Chen et al., 2012, Li et al., 2023] to generate a safe and efficient path for the next 10 seconds.

The above applications reveal a growing gap between classical theory and practical scenarios: classical theory pursues optimal performance guarantees when the iteration number T approaches infinity, and the resulting designs may not be well-suited in scenarios with a small finite T (see Figure 1 (a) as an illustration). This raises the new question of optimal hyperparameter design for a fixed and finite iteration budget.

In this work, we introduce the framework of *finite horizon optimization*, which focus on optimizing the algorithmic behaviors under a strict iteration budget. We will review some existing approaches that fall within this finite horizon framework, and also introduce several practical problems that could be improved using this framework. In the main body of this work, we will apply the finite horizon framework to linear programming (LP) [Kantorovich, 1960, Schrijver, 1998, Dantzig, 2002, Luenberger and Ye, 1984, Boyd and Vandenberghe, 2004]. We study LP because LP (and its variants) frequently emerge in engineering scenarios where solvers must operate under strict iteration limit (some examples are provided later in Section 1.2). We will primarily work on a most simple yet fundamental algorithm to solve LP, namely, the primal-dual method. We aim to design a new stepsize rule for the primal-dual method, tailored for the scenarios where the total iteration budget T is fixed and finite.

Perhaps a bit surprisingly, we find that: if we abandon the pursuit of asymptotic performance and instead focus on how the algorithm performs within a finite number of iterations, the primal-dual method can be substantially accelerated by merely changing its stepsize design. We provide an illustration in Figure 1 (b). This figure visualizes the augmented Lagrangian function of a simple LP, and the saddle point of this function is the optimal primal-dual solution to the LP. When the stepsize rule is particularly designed for a total iteration budget $T = 2$, we find that the primal-dual method can reach the saddle point in 2 steps, while

the conventional constant stepsize cannot solve the problem until > 200 steps². Note that such acceleration is reached without changing the algorithm, e.g., storing extra building blocks like momentum [Nesterov et al., 2018]. We summarize our contribution as follows.

- We introduce the framework of *finite horizon optimization*, which focuses on optimizing algorithmic performance under a strict iteration budget. We review existing approaches that fall within this framework and present several practical problems that could benefit from this methodology.
- We introduce Finite Horizon stepsize rule for the primal-dual method for solving LP, especially for the scenarios where the total iteration budget T is fixed and finite. The main challenge in designing this stepsize rule is controlling the singular values of T cumulative product of *non-symmetric* matrices, which appears to be a highly nonconvex problem, and there is very few helpful tool. In the special case of the primal-dual method, we find that the optimal stepsize design problem admits hidden convexity and we propose a convex semidefinite programming (SDP) reformulation. This reformulation involves only matrix constraints of size 4×4 and can be solved efficiently by SDP solvers in negligible computation time. A theoretical acceleration guarantee is also provided at the pre-fixed T -th iteration, but with no asymptotic guarantee.
- We numerically verify the effectiveness of Finite Horizon stepsize rule on real-world LP datasets. On the Netlib LP benchmark with more than 90 real-world instances, our stepsize rule archives an average $3.9\times$ speed-up over the optimal constant stepsize, saving 75% wall-clock time to achieve the same level of precision. Our results reveal substantial room for improvement when we abandon asymptotic guarantees, and instead focus on the performance under finite horizon. We highlight that the benefits are shown not only in worst-case theory, but also manifest immediately in real-world problems.

1.1 Notations

- **Matrix-related notations.** Given a matrix $X \in \mathbb{R}^{m \times n}$, we denote X^\top as the transpose of X . Similarly, for $X \in \mathbb{C}^{m \times n}$, we denote X^H as hermitian of X . We write the singular value decomposition (SVD) of X as $X = U\Sigma V^\top = \sum_{i=1}^m \sigma_i u_i v_i^\top$, where $U \in \mathbb{R}^{m \times m}$, $V \in \mathbb{R}^{n \times n}$ are orthonormal matrices and $u_i \in \mathbb{R}^m$, $v_i \in \mathbb{R}^n$ are the i -th column of U and V , respectively; Σ is the rectangular diagonal matrix with diagonal entries $\sigma_1 \geq \sigma_2 \geq \dots \geq \sigma_m \geq 0$. We also use $\sigma(X)$ to denote the set of singular values of X . We denote $\|X\|_{\text{op}}$ as the spectral norm (a.k.a., operator norm) of X , i.e., the square root of the maximal eigenvalue of $X^\top X$, or equivalently, the maximal singular value σ_1 of X . When X is a square matrix with $m = n$, we use $\lambda(X)$ to denote the set of eigenvalues of X . we denote $\rho(X) := \max \{|\lambda(X)|\}$ as the spectral radius of X . When X is positive semi-definite (PSD), we use $\kappa = \frac{\lambda_{\max}(X)}{\lambda_{\min}^+(X)}$ to denote the condition number of X , where $\lambda_{\max}(X)$, $\lambda_{\min}^+(X)$ are the maximal eigenvalue and the smallest non-zero eigenvalue, respectively. We use $\text{null}(X)$ to denote the null space of X . We use $I_{n \times n}$ and $0_{n \times n}$ to denote the identity matrix and the zero matrix of size $n \times n$.
- **Algorithm-related notations.** We say an algorithm has complexity $\tilde{\mathcal{O}}(C)$ or $\mathcal{O}(C \log(1/\epsilon))$ if it takes (at most) $\mathcal{O}(C \log(1/\epsilon))$ iterations to achieve error $\frac{\text{dist}(z, \mathcal{Z}^*)}{\text{dist}(z^0, \mathcal{Z}^*)} \leq \epsilon$, where $\text{dist}(\cdot, \cdot)$ denotes the Euclidean distance, z is the decision variable, z^0 is the initial point, \mathcal{Z}^* is the solution set. Similarly, we say an algorithm has complexity $\tilde{\Omega}(C)$ or $\Omega(C \log(1/\epsilon))$ if it takes (at least) $\Omega(C \log(1/\epsilon))$ iterations to achieve error $\frac{\text{dist}(z, \mathcal{Z}^*)}{\text{dist}(z^0, \mathcal{Z}^*)} \leq \epsilon$.
- **Other notations.** We use $[n]$ to denote the index set $\{1, 2, \dots, n\}$. For a vector $x \in \mathbb{R}^n$, $\|x\|_2$ denotes the Euclidean norm of x , x^+ and x^- denote the vector of positive parts and negative parts of x , respectively. That is: the components of x^+ and x^- are $(x^+)_i = \max \{x_i, 0\}$ and $(x^-)_i = \max \{-x_i, 0\}$ for $i \in [n]$.

²We provide the detailed curves of optimality gap and the stepsize rules in Appendix A.

1.2 General Framework of Finite Horizon Optimization

We now state the general framework for finite horizon optimization. Suppose we are given a function class \mathcal{F} and an iterative algorithm $\mathcal{A}(x, \theta)$, where $x \in \mathcal{X}$ is the optimization variable and $\theta \in \Theta$ is the algorithmic configuration (e.g., hyperparameters, or building components). We define the performance measurement $\epsilon(x)$ to be a nonnegative function of x . We aim to adjust the algorithmic configuration θ to optimize the worst-case performance of the algorithm after T iterations, where T is pre-determined. The general formulation of finite horizon optimization is shown below.

$$\begin{aligned}
 & \min_{\theta \in \Theta} \max_{f \in \mathcal{F}, x_0 \in \mathcal{X}} \epsilon(x_T) \\
 & \text{s.t. } x_T = \mathcal{A}(x_{T-1}, \theta), \\
 & \quad x_{T-1} = \mathcal{A}(x_{T-2}, \theta), \\
 & \quad \vdots \\
 & \quad x_1 = \mathcal{A}(x_0, \theta).
 \end{aligned} \tag{1}$$

One may also easily generalize this formulation to the ‘‘average case in \mathcal{F} ’’ instead of ‘‘worst case in \mathcal{F} ’’, or ‘‘average performance within T iterations’’ instead of ‘‘the final performance at the T -th step’’. We now provide some concrete examples that belong to (1) (**Example 1, 2**), as well as some examples that can be fit into (1) in the future (**Example 3, 4, 5**).

Example 1: stepsize design of GD for unconstrained minimization. Formulation (1) can be applied to select the optimal stepsize rules of GD after T iterations, where T is pre-determined. The stepsize selection problem can be modeled as follows.

$$\begin{aligned}
 & \min_{\eta_0, \dots, \eta_{T-1}} \max_{f \in \mathcal{F}, x_0 \in \mathbb{R}^d} \epsilon(x_T) \\
 & \text{s.t. } x_T = x_{T-1} - \eta_{T-1} \nabla f(x_{T-1}), \\
 & \quad x_{T-1} = x_{T-2} - \eta_{T-2} \nabla f(x_{T-2}), \\
 & \quad \vdots \\
 & \quad x_1 = x_0 - \eta_0 \nabla f(x_0).
 \end{aligned} \tag{2}$$

Solving Problem (2) for a general \mathcal{F} remains challenging. Fortunately, there have been some exciting breakthroughs for certain special classes of \mathcal{F} . The pioneer work [Young, 1953] solved (2) when \mathcal{F} is the μ -strongly-convex L -smooth *quadratic* functions and $\epsilon(x) := \|x - x^*\|_2^2$ denotes the distance to optimal solution. Perhaps a bit surprisingly, the optimal $(\eta_0, \dots, \eta_{T-1})$ in this case has the following closed-form solution.

$$\eta_t = 2 \left((L + \mu) + (L - \mu) \cos \left(\left(t - \frac{1}{2} \right) \frac{\pi}{T} \right) \right)^{-1}, \quad t = 0, \dots, T-1. \tag{3}$$

Eq. (3) is related to the inverse of the roots of the T -th order Chebyshev polynomial. We will refer to (3) as Young’s stepsize. The derivation of Young’s stepsize relies on a special connection between quadratic minimization and the minimax polynomial theory. The proof is presented in recent works [Altschuler, 2018, Pedregosa, 2020, d’Aspremont et al., 2021]. With Young’s stepsize, the optimal value of $\epsilon(x_T)$ satisfies $\epsilon(x_T) \leq 2 \left(1 - \frac{2}{\sqrt{\kappa+1}} \right)^T$, which can be translated into the complexity of $\tilde{O}(\sqrt{\kappa})$. Note that the square-root dependency on κ matches the lower bound of first-order methods [Nesterov et al., 2018], which achieves acceleration over the complexity lower bound of constant stepsize $\tilde{\Omega}(\kappa)$. It is worth mentioning that Young’s stepsize is the first non-constant stepsize rule that achieves acceleration over the constant stepsize. It is also the first stepsize rule that helps vanilla GD achieve the optimal dependency on κ without modifying the algorithm (e.g., introducing extra building blocks such as momentum [Polyak, 1964, Nesterov et al., 2018]).

Recently, researchers have tried to design better stepsize rule of GD beyond the quadratic case. Now let \mathcal{F} be the generic L -smooth convex functions and $\epsilon(x_t) := f(x_t) - \inf f$ and we still try to solve (2). Unfortunately, the optimal $(\eta_0, \dots, \eta_{T-1})$ does not admit a closed-form analytic expression in this case. Rather, [Das Gupta et al. \[2024\]](#) pointed out that (2) can be reformulated as a nonconvex QCQP and proposed to solve it via branch-and-bound methods. They then discovered the optimal stepsize rule for $T \leq 25$. Similar stepsize rule for $T \leq 127$ are also discovered by "brute force searching" [[Grimmer et al., 2023](#)]. Although these stepsize rules do not reach the lower bound complexity like Young's stepsize, they still achieve highly non-trivial improvement over constant stepsize.

We emphasize that the complexity of the aforementioned stepsize rules only holds at T -th step but not at any other iterations, so it does not have asymptotic guarantees like constant stepsize. These stepsize rules serve as examples that: GD can be substantially accelerated if we abandon the asymptotic guarantees and focus on the performance within T iterations.

Example 2: Algorithm Unrolling (AU). AU is a data-driven approach that employs a finite-depth neural network to learn the behavior of a specific algorithm after an infinite number of iterations (e.g., [[Gregor and LeCun, 2010](#), [Sun et al., 2016, 2018](#), [Yang et al., 2018](#), [Adler and Öktem, 2018](#), [Monga et al., 2021](#), [Chen et al., 2022](#), [Li et al., 2024](#)]). We now interpolate AU under the framework of finite horizon optimization. We denote the t -th layer of a neural network as $\varphi_t(x, W_t)$, where x is the input, W_t is the trainable weight, $t = 0, \dots, T-1$. Given a neural network architecture with T total layers, AU aims to train this neural network to solve the following problem.

$$\begin{aligned} \min_{W_0, \dots, W_{T-1}} \sum_{f \in \mathcal{F}} \sum_{x_0 \in \mathcal{X}} \|x_T - x^*(f, x_0)\|_2^2 \\ \text{s.t. } x_T = \varphi_{T-1}(x_{T-1}, W_{T-1}), \\ x_{T-1} = \varphi_{T-2}(x_{T-2}, W_{T-2}), \\ \vdots \\ x_1 = \varphi_0(x_0, W_0), \end{aligned} \tag{4}$$

where $x^*(f, x_0) = \lim_{n \rightarrow \infty} \underbrace{\mathcal{A}(\mathcal{A}(\dots \mathcal{A}(f, x_0)))}_{n \text{ iterations}}$ denotes the output of the target algorithm on f and

initialization x_0 . With an appropriately designed neural network architecture, a diverse collection of training instances from \mathcal{F} , and sufficient training of the weights $\{W_t\}_{t=0}^{T-1}$, the trained neural network can achieve performance comparable to \mathcal{A} on test problem instances, all while significantly reducing computational costs. For instance, a neural network with $T = 4$ layers can perform on par with ≥ 1000 iterations of Primal-Dual Hybrid Gradient algorithm (PDHG) on real-world LP benchmark, which helps reduce $\geq 45\%$ wall-clock running time [[Li et al., 2024](#)].

From the perspective of finite horizon optimization, the objective of AU (4) is closely related to the objective in (1): both (1) and (4) aims to accelerate certain algorithm under finite T , up to the minor difference that "worst case in \mathcal{F} " in (1) is changed to "average case in \mathcal{F} " in (4). We believe AU serves as an example that traditional algorithms can be substantially improved under the finite horizon framework, e.g., such as through re-parametrization using finite-depth neural networks.

In the sequel, we provide some practical engineering problems where there is a strict upper bound on the total iteration number T . We believe there is substantial room for improvement if we re-design the relevant algorithms under the finite horizon framework (1).

Example 3: Weighted Sum Mean Square Error Minimization (WMMSE). WMMSE [[Shi et al., 2011](#)] is a popular optimization framework for efficient resource allocation in multiple-input multiple-output (MIMO) wireless communication systems. The goal of WMMSE is to maximize the weighted sum rate (WSR) of the system, which is a common objective in wireless networks to balance fairness and throughput among users. However, directly optimizing the WSR is often challenging due to its non-convex nature. WMMSE addresses

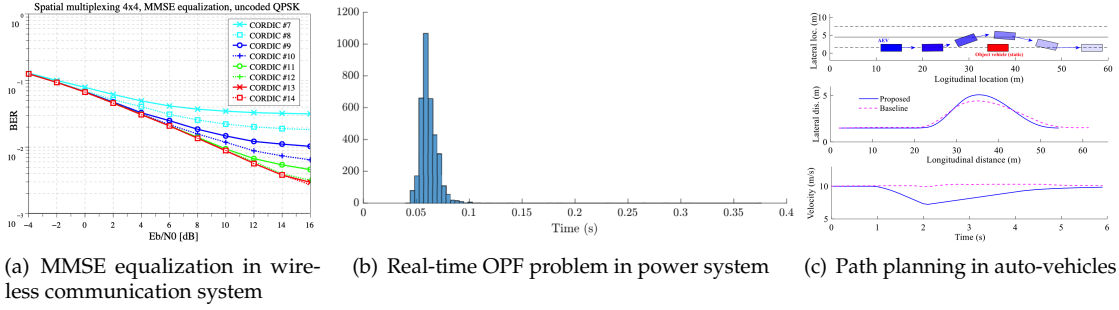


Figure 2: Some practical applications with strict iteration budget for solvers. **(a):** Figure 4 in [Boher et al., 2008]. Performance of MMSE equalization algorithms in MIMO wireless communication systems after $\#x$ number of iterations. The maximal affordable iteration number is 14. **(b)** Figure 5 in [Tang et al., 2017]. For real-time OPF problems in power system, the average running time for iterative algorithms is 0.062 seconds with 12 iterations, and the maximum is 0.376 seconds. **(c)** Figure 6 in [Li et al., 2023]. The path planner of autonomous vehicles needs to make decisions in 20 ms to avoid collision in the next 10 seconds.

this by introducing an additional weight matrix and lifting the problem into a higher dimensional space, where the problem has a more tractable form. The objective of WMMSE is formulated as follows.

$$\begin{aligned}
 \min_{\{W_i, V_i, U_i\}_{i=1}^I} & \sum_{i=1}^I \alpha_i (\text{Tr}(W_i E(U_i, V_i)) - \log \det(W_i)) \\
 \text{s.t.} & \sum_{i=1}^I \text{Tr}(V_i V_i^H) \leq P_{\max},
 \end{aligned} \tag{5}$$

where $W_i \in \mathbb{R}^{d_i \times d_i}$ is a positive-semidefinite weight matrix for receiver i ; $V_i \in \mathbb{C}^{M \times d_i}$ and $U_i \in \mathbb{C}^{N_i \times d_i}$ is the beamformer and decoder for receiver i , respectively; M and N_i are the number transmit antennas of the base station and receive antennas of user i , respectively; α_i is the priority of user i in the system; $E(U_i, V_i)$ is a quadratic function in U_i and V_i ; P_{\max} is the power budget of transmitter. More descriptions can be seen in [Shi et al., 2011]. Problem (5) is then solved iteratively by the WMMSE algorithm, which cyclically update $\{W_i, V_i, U_i\}_{i=1}^I$ in a block-coordinate-descent fashion. The authors established the convergence guarantee of the WMMSE algorithm by leveraging the observation that the optimization problem in (5) is convex with respect to each individual variable when the other variables are held fixed.

Here, we highlight the relation between WMMSE and the finite horizon framework. To deploy the WMMSE framework in a real-time communication system, the WMMSE algorithm needs to find good solutions of beamformer V_i and decoder U_i within **4 iterations** (in Single-Input-Single-Output case) or **10 iterations** (in MIMO case) [Shi et al., 2011, Figure 1]. Otherwise, the users will suffer from high-latency communications. Such requirement is ubiquitous in wireless communication systems. Another similar example is presented in Figure 2 (a), where the iterative algorithms in the MIMO system are only allowed to operate **within 14 iterations**. This calls for the need to re-design the WMMSE algorithm under the finite horizon framework (1) and boost performance within strict constraints of total iteration number T . Nevertheless, WMMSE is not the main focus of this script, and the relevant progress will be reported elsewhere.

Example 4: Optimal power flow (OPF) problem. OPF is a fundamental problem in power systems to determine the most economical and secure way to distribute electrical power while satisfying network constraints [Chatzivasileiadis, 2018]. DC-OPF problem is a linear approximations of the actual nonlinear OPF problem³, and it is widely used for real-time operational planning and control due to its computational efficiency and ability to handle large-scale networks [Frank et al., 2012]. DC-OPF minimizes the total generation cost subject to the limits of generator operation, the power balance equation, and the transmission line capacity constraints [Christie et al., 2000]. DC-OPF admits an LP formulation as follows [Pan, 2021].

³The name of DC-OPF is a bit misleading, as this method does not assume the use of direct current (as opposed to alternating current). Rather, it is merely a linearization of AC-OPF problem, which is another name for the original OPF problem [Mones, 2021].

$$\begin{aligned}
& \min_{\{P_{Gi}\}_{i=1}^{N_{\text{gen}}}, \{\theta_i\}_{i=1}^{N_{\text{bus}}}} \sum_{i=1}^{N_{\text{gen}}} c_i P_{Gi} \\
& \text{s.t. } P_{Gi}^{\min} \leq P_{Gi} \leq P_{Gi}^{\max}, i = 1, 2, \dots, N_{\text{bus}}, \\
& \sum_{j=1}^{N_{\text{bus}}} B_{i,j} \theta_j = P_{Gi} - P_{Di}, i = 1, 2, \dots, N_{\text{bus}}, \\
& \frac{1}{x_{ij}} (\theta_i - \theta_j) \leq P_{ij}^{\max}, i, j = 1, 2, \dots, N_{\text{bus}},
\end{aligned} \tag{6}$$

where N_{gen} denotes the number of generators and N_{bus} is the number of buses. P_{Gi} (and P_{Di}) denotes the power output (and consumption) of the generator in the i -th bus. P_{Gi}^{\min} and P_{Gi}^{\max} are the output limits of generators in the i -th bus, respectively. θ_i is the phase angle at the i -th bus. $B_{i,j}$ and $x_{i,j}$ are constant terms from the power balance equations. More descriptions can be seen in [Pan, 2021].

We highlight the relation between OPF problems and the finite horizon framework. In practice, LP solvers must return their solutions to DC-OPF **with far less than 1 second**; otherwise, it will be too slow to adjust the system's operating points in response to *real-time* changes in renewable power injection [Zhang et al., 2021, Babaeinejadsarookolae et al., 2019, Tang et al., 2017]. Unfortunately, This makes most standard solvers incompetent in these scenarios [Tang et al., 2017]. Currently, the average algorithm running time for real-time OPF is **0.062 second with 12 iterations** [Tang et al., 2017] (see Figure 2 below). Tang et al. [2017] also pointed out that "*most algorithms in the literature must wait until the iteration has converged because the intermediate iterates typically do not satisfy power flow equations and are not implementable.*" They also pointed out that the traditional algorithms will be "*inadequate for future power grids*", and we need "*real-time OPF algorithms*" that can respond quickly to network changes and maintain (sub)optimality."

To sum up, future power system requires algorithms to operate within a strict upper bound on the total iteration number T , and this raises the question of optimal algorithm design under framework (1).

Example 5: Path planning in autonomous vehicles. Path planning is a critical component of autonomous vehicles, responsible for determining the optimal route of the vehicle within a certain time window. A qualified path planner must generate trajectories that allow the vehicle to reach destinations, avoid obstacles, and minimize fuel consumption, all while taking into account for environmental constraints such as buildings, pedestrians, and other moving vehicles. The path planner must make decisions every few seconds to ensure a safe and efficient path in real-time [Culligan, 2006]. Typically, the search for a good planner can be formulated as various optimization problems including LP [Chasparis and Shamma, 2005, Chen et al., 2012, Kiessling et al., 2022], mix-integer LP (MILP) [Culligan, 2006, Toupet, 2006], convex QCQP [Subosits and Gerdes, 2019], and others [Dolgov et al., 2008]. For example, the following LP often arises in time-optimal motion planning [Kiessling et al., 2022].

$$\begin{aligned}
& \min_{w \in \mathbb{R}^{N_w}} c^\top w \\
& \text{s.t. } Cw + G^\top P_y (w - \hat{w}) = 0, \\
& Aw + b \leq 0, \\
& \|P_y (w - \hat{w})\|_\infty \leq \Delta,
\end{aligned} \tag{7}$$

where the optimization variable w is the concatenation of state, control, and slack variables. More introduction for w and the physical meanings of constant terms including $c, C, G, P_y, \hat{w}, A, b, \Delta$ can be seen in [Kiessling et al., 2022]. Here, we highlight the relation between the autonomous path planner and the finite horizon framework. To generate a safe and efficient path in real-time, the sub-problems of LP (7) must be solved in **within 10 ms** [Chen et al., 2012, Table VI]. Similarly, the MILP formulation in [Culligan, 2006] and [Yu and Fan, 2024, Table 1] need to be solved in **within 100 ms** to get the plan for the next 10 seconds; the

convex QCQP in [Subosits and Gerdes, 2019] needs to be solved in **within 20 ms** for the plan in the next 10 seconds (Figure 2 (c)); the MIQP in [Qian et al., 2016, Table II] needs to be solved in **within 228 ms**. All these strict constraints on operation time post an upper bound on the total iteration number T .

Goal. Motivated by the examples above, we aim to design new stepsize rules for LP algorithms under the finite horizon framework (1). We study LP because LP (and its variants) frequently arise in engineering scenarios with strict iteration budget constraints for solvers, such as **Example 4** and **5** above. As an initial attempt, we will work on a most simple yet fundamental algorithm: the primal-dual method. We will show that the primal-dual method can be accelerated by about $3.9\times$ if the stepsize rules are re-designed using formulation (1). The acceleration comes at a price of sacrificing asymptotic guarantees, but as argued above, this trade-off is inconsequential for the a wide range of applications.

It would be intriguing to apply framework (1) to more advanced methods such as the momentum or the preconditioned variants of primal-dual method [Applegate et al., 2021], where we believe substantial potential for improvement remains. Given the technical complexity involved in the analysis of the primal-dual method, we will concentrate on this algorithm for now and defer the extensions to future research.

Challenges. Our stepsize design of the primal-dual method is inspired by the seminal work [Young, 1953] in **Example 1**. Young [1953] focused on GD for quadratic functions, and we provide a (rather non-trivial) extension of their idea to the primal-dual method. There are at least two-fold challenges.

- **First: non-symmetric update matrix.** The primal-dual method is driven by a *non-symmetric* update matrix (i.e., M is non-symmetric in (32)), whereas GD for quadratic is driven by a symmetric update matrix (i.e., Hessian). We highlight that for non-symmetric matrices, their singular values are usually largely different from their eigenvalues. This posts the following difficulties. First, most existing stepsize designs of GD including [Young, 1953] focus on controlling Hessian eigenvalues. Since we aim to control singular values, these eigenvalue-based approaches cannot be directly applied. Second, in general, there are very few tools to analyze the singular values of non-symmetric matrices. Similar difficulties are also reported in [Kittaneh, 2006, Sun et al., 2020, Sun and Ye, 2021].
- **Second: non-asymptotic analysis.** Since we focus on the *non-asymptotic* regime with finite T , we cannot use any asymptotic properties of the singular value spectrum. For instance, we cannot apply the asymptotic relation between singular values and eigenvalues [Saad, 2003] or any similar theoretical results. To our knowledge, there are very few helpful tools in this non-asymptotic regime.

We present our stepsize rule in **Algorithm 1**. We address the above two challenges by uncovering the hidden convexity inherent in (1) for any T , a property uniquely brought up by the primal-dual method. We then propose a convex SDP reformulation of (1) and numerically search for the desired stepsize. The SDP only involves matrices with size 4×4 and can be solved efficiently by modern solvers. While having an (exact) convex reformulation may not be as convenient as having a closed-form solution as in (3) [Young, 1953], it is still better news compared to the (exact) nonconvex reformulation for GD stepsize [Das Gupta et al., 2024]. We introduce the detailed derivation of **Algorithm 1** in the next section.

Algorithm 1 Finite Horizon stepsize rule

- 1: Input the total iteration budget T .
 - 2: Input the smallest & largest singular value of A (the constraint matrix in LP), denoted as μ, L .
 - 3: Get n_{sample} evenly spaced numbers over $[\mu, L]$, denoted as $\{\sigma_i\}_{i=1}^{n_{\text{sample}}}$.
 - 4: Formulate the SDP (31) using $\{\sigma_i\}_{i=1}^{n_{\text{sample}}}$ and T . Solve it using the Interior Point Methods, return the optimal solution $\{a_t\}_{t=1}^T$.
 - 5: Find the roots of the polynomial $p(x) = 1 + a_1x + a_2x^2 \cdots + a_Tx^T$ using the algorithm in [Horn and Johnson, 2012], denoted as $\{r_t\}_{t=1}^T$.
 - 6: Calculate $\eta_t = 1/r_t$, for $t = [T]$.
 - 7: Return $\{\eta_t\}_{t=1}^T$ as the stepsize rule.
-

2 Main Methods

2.1 LP Formulation and Algorithms

We consider the standard form of LP as follows.

$$\begin{aligned} \min_{x \in \mathbb{R}^n} \quad & c^\top x \\ \text{s.t.} \quad & Ax = b \\ & x \geq 0, \end{aligned} \tag{8}$$

where $c \in \mathbb{R}^n, b \in \mathbb{R}^m$ and we assume $A \in \mathbb{R}^{m \times n}$ is full rank and $m \leq n$. The singular values of A satisfy $\sigma(A) \subseteq [\mu, L]$, where $\mu, L > 0$. We consider the primal-dual form of (8):

$$\min_{x \geq 0} \max_{y \in \mathbb{R}^m} \mathcal{L}_\beta(x, y) := c^\top x + y^\top (Ax - b) + \frac{\beta}{2} \|Ax - b\|_2^2, \tag{9}$$

where $\mathcal{L}_\beta(x, y)$ is the augmented Lagrangian function. To solve the primal-dual formulation of LP (9), a most simple first-order method (FOM) is the primal-dual method, or equivalently, the projected gradient descent-ascent method (GDA):

$$\begin{cases} x^{t+1} = (x^t - \eta_t (c + A^\top y^t + \beta A^\top (Ax^t - b)))^+ \\ y^{t+1} = y^t + \eta_t (Ax^t - b), \end{cases} \tag{10}$$

where $(\cdot)^+$ operator is the projection onto the non-negative orthant and is cheap to implement. We denote η_t as the stepsize at t -th step for the primal and dual update. In this work, we will use the same stepsize η_t for both primal and dual updates. We ask the following question:

Given a finite iteration budget T , how to find the optimal stepsize rule $\{\eta_t\}_{t=1}^T$ of (10) for these T iterations?

2.2 Finite Horizon Stepsize Rule

We now design Finite Horizon stepsize rule for the primal-dual method (10). We first rewrite the primal update as follows.

$$\begin{aligned} x^{t+1} - x^* &= \left(x^t - \eta_t \left(c + A^\top y^t + \beta A^\top (Ax^t - b) \right) \right)^+ - x^* \\ &\stackrel{(i)}{=} \left((x^t - x^*) - \eta_t \left(c + A^\top y^t + \beta A^\top A(x^t - x^*) \right) \right)^+, \\ &\stackrel{(ii)}{=} \left((x^t - x^*) - \eta_t \left(A^\top (y^t - y^*) + \beta A^\top A(x^t - x^*) \right) \right)^+, \\ &= \left((I - \eta_t \beta A^\top A)(x^t - x^*) - \eta_t \left(A^\top (y^t - y^*) \right) \right)^+, \end{aligned} \tag{11}$$

where x^* and y^* are optimal primal and dual solutions, respectively; (i) is due to: $(x^*)^+ = x^*, Ax^* = b$. (ii) is due to the KKT condition $A^\top y^* = -c$. Similarly, we rewrite the dual update as follows.

$$y^{t+1} - y^* = y^t - y^* + \eta_t A(x - x^*). \tag{12}$$

Define $z = [(x)^\top, (y)^\top]^\top \in \mathbb{R}^{(n+m)}$, the update equations (11) and (12) can be rewritten as

$$z^{t+1} - z^* = P_t \begin{bmatrix} (I_{n \times n} - \eta_t \beta A^\top A) & -\eta_t A^\top \\ \eta_t A & I_{m \times m} \end{bmatrix} (z^t - z^*), \tag{13}$$

where P_t is a diagonal matrix defined as follows:

$$P_t = \begin{bmatrix} p_{t,1} & \cdots & 0 & 0 \\ & \ddots & & \\ 0 & \cdots & p_{t,n} & 0 \\ 0 & \cdots & 0 & I_{m \times m} \end{bmatrix} \in \mathbb{R}^{(n+m) \times (n+m)}, p_{t,i} = \begin{cases} 0 & \text{if } x_{t,i} < 0 \\ 1 & \text{otherwise.} \end{cases} \quad (14)$$

Define

$$M = \begin{bmatrix} \beta A^\top A & A^\top \\ -A & 0_{m \times m} \end{bmatrix}, \quad (15)$$

then the update equation (13) can be further rewritten as

$$z^{t+1} - z^* = P_t(I - \eta_t M)(z^t - z^*) \quad (16)$$

$$= P_t(I - \eta_t M)P_{t-1}(I - \eta_{t-1}M) \cdots P_1(I - \eta_1 M)(z^0 - z^*). \quad (17)$$

Given a class of LP instances with $\sigma(A) \subseteq [\mu, L]$, we aim to find the optimal stepsize rule $\{\eta_t\}_{t=1}^T$ for T total iterations, where $T > 0$ is a finite integer. In particular, we aim to minimize the "worst-case" distance to the optimal solution at iteration T . Here, the "worst-case" is in the sense of LP instance A and initial point z^0 . This gives rise to the following optimization problem.

$$\min_{\eta_1, \dots, \eta_T} \max_{A, s, t, \sigma(A) \subseteq [\mu, L], z \notin \mathcal{Z}^*} \frac{\|P_T(I - \eta_T M)P_{T-1}(I - \eta_{T-1}M) \cdots P_1(I - \eta_1 M)(z - z^*)\|_2}{\|z - z^*\|_2}, \quad (18)$$

where $\mathcal{Z}^* = \{z; z \text{ is the optimal primal-dual solution of (8), } z \in \text{null}(M)\}$, and z^* is a closest point in \mathcal{Z}^* to z . To solve (18), one immediate obstacle lies in how to handle the projection matrices P_t . There are at least two challenges. **First**, the realization of P_t depends on the specific algorithmic trajectory, which is almost unpredictable in the worst-case-based formulation (18). **Second**, P_t does not commute with M , i.e., $P_t(I - \eta_t M)$ does not share the same singular vectors with $(I - \eta_t M)$. In the worst case, the singular vectors of the update system changes at every step, making it hard to analyze.

In this work, we view the projection P_t as random projection matrices, i.e., $p_{t,i} \stackrel{\text{i.i.d.}}{\sim} \text{Bernoulli}(1 - p_{\text{proj}})$, and we consider the expected output of the random projection at iteration T :

$$\mathbb{E} [z^T - z^*] = \mathbb{E}_{P_1, \dots, P_T} [P_T(I - \eta_T M)P_{T-1}(I - \eta_{T-1}M) \cdots P_1(I - \eta_1 M)(z^0 - z^*)] \quad (19)$$

$$= P(I - \eta_T M)P(I - \eta_{T-1}M) \cdots P(I - \eta_1 M)(z^0 - z^*), \quad (20)$$

where

$$P = \begin{bmatrix} 1 - p_{\text{proj}} & \cdots & 0 & 0 \\ & \ddots & & \\ 0 & \cdots & 1 - p_{\text{proj}} & 0 \\ 0 & \cdots & 0 & I_{m \times m} \end{bmatrix} \in \mathbb{R}^{(n+m) \times (n+m)}. \quad (21)$$

We now rewrite the expected output. We first define $\tilde{I} \in \mathbb{R}^{(n+m) \times (n+m)}$ and $\tilde{M} \in \mathbb{R}^{(n+m) \times (n+m)}$ as follows.

$$\tilde{I} = \begin{bmatrix} I_{n \times n} & 0_{n \times m} \\ 0_{m \times n} & 0_{m \times m} \end{bmatrix} \in \mathbb{R}^{(n+m) \times (n+m)}, \tilde{M} = \tilde{I}M. \quad (22)$$

Then we have

$$\begin{aligned}
& \mathbb{E}_{P_1, \dots, P_T} [P_T(I - \eta_T M) \cdots P_1(I - \eta_1 M)] \\
= & P(I - \eta_T M) \cdots P(I - \eta_1 M) \tag{23} \\
= & (I - \eta_T M - p_{\text{proj}}(\tilde{I} - \eta_T \tilde{M})) \cdots (I - \eta_1 M - p_{\text{proj}}(\tilde{I} - \eta_1 \tilde{M})) \\
= & (I - \eta_T M) \cdots (I - \eta_1 M) \\
& + p_{\text{proj}} \sum_{t=1}^T (I - \eta_T M) \cdots (I - \eta_{t+1} M) (\tilde{I} - \eta_t \tilde{M}) (I - \eta_{t-1} M) \cdots (I - \eta_1 M) \\
& + p_{\text{proj}}^2 \sum_{1 \leq i, j \leq T} (I - \eta_T M) \cdots (I - \eta_{j+1} M) (\tilde{I} - \eta_j \tilde{M}) (I - \eta_{j-1} M) \cdots (I - \eta_{i+1} M) (\tilde{I} - \eta_i \tilde{M}) (I - \eta_{i-1} M) \cdots (I - \eta_1 M) \\
& + \cdots \\
& + p_{\text{proj}}^T (\tilde{I} - \eta_T \tilde{M}) \cdots (\tilde{I} - \eta_1 \tilde{M}) \\
:= & \underbrace{(I - \eta_T M) \cdots (I - \eta_1 M)}_{(a)} + \underbrace{p_{\text{proj}} \text{Residue}}_{(b)}. \tag{24}
\end{aligned}$$

In the sequel, we focus on optimizing the leading term (a). We focus on (a) because: we numerically find that p_{proj} is small when initializing z^0 in the positive orthant, and the resulting p_{proj} is usually ≤ 0.1 . Further, when p_{proj} is small, we find that the operator norm of (23) is close to the operator norm of (a). As such, term (a) usually plays a more crucial role in the overall convergence rate. We relegate the numerical evidence in Section 5. Now we focus on term (a) and solve the following problem (25).

$$\min_{\eta_1, \dots, \eta_T} \max_{A, s, t, \sigma(A) \subseteq [\mu, L], z \notin \mathcal{Z}^*} \frac{\|(I - \eta_T M)(I - \eta_{T-1} M) \cdots (I - \eta_1 M)(z - z^*)\|_2}{\|z - z^*\|_2}. \tag{25}$$

Challenges for solving (25). We note that (25) is non-trivial to solve. There are at least three challenges.

- **C1: Nonconvexity.** The optimization variable η_1, \dots, η_T appears in (25) as a product form. This makes the objective function nonconvex.
- **C2: Non-symmetric M .** Eq. (25) involves controlling the singular values of $(I - \eta_T M) \cdots (I - \eta_1 M)$, which is the product of non-symmetric matrices. It is worth mentioning that: for non-symmetric matrices, their singular values are usually largely different from their eigenvalues, and there is no clear relation between these two. This posts the following difficulties. First, most existing stepsize design of GD (e.g., [Young, 1953]) focus on controlling eigenvalues of symmetric matrices (Hessian). Since we aim to control singular values, which are *not* equal to eigenvalues anymore in the non-symmetric case, these eigenvalue-based approaches cannot be directly applied. Second, in general, there are very few tools to analyze non-symmetric matrices (actually, both singular values and eigenvalues of non-symmetric matrices are difficult topics with very limited results). Similar difficulties in analyzing non-symmetric matrices are also reported in [Kittaneh, 2006, Sun et al., 2020, Sun and Ye, 2021].

Here, we post a simple example to illustrate that: for non-symmetric matrices, the gap between singular values and eigenvalues can be arbitrarily large. Consider $M = \begin{pmatrix} 0 & \alpha \\ 0 & 0 \end{pmatrix}$, its eigenvalues are 0 with multiplicity 2, while its maximal singular values equals $|\alpha|$, which could be unbounded as $\alpha \rightarrow \infty$. This huge gap makes all eigenvalue-based methods inapplicable.

- **C3: Non-asymptotic analysis.** One possible solution to C2 is to transform singular values into eigenvalues and then resort to the eigenvalue analysis in [Young, 1953]. Unfortunately, for non-symmetric matrices, most existing relations between singular values and eigenvalues only apply in the asymptotic sense. For instance, [Saad, 2003, Theorem 1.12] states that $\lim_{T \rightarrow \infty} \sigma_1(M^T)^{1/T} = |\lambda_1(M)|$. In indeed, we have $\lim_{T \rightarrow \infty} \sigma_1(M^T)^{1/T} = 0$ for the 2×2 example above. However, in the non-asymptotic regime, the gap between singular values and eigenvalues can still be arbitrarily large. In the non-asymptotic regime, one potential approach is to use the symmetrization trick, i.e., to analyze the eigenvalues of $M^\top M$. However,

this is still not easy since the eigenbasis of M is *not* orthonormal, and thus it is unclear whether we can diagonalize $M^\top M$ to extract its eigenvalues.

Perhaps a bit surprisingly, we find (25) admits hidden convexity for any T under proper changes of variables. We will show that (25) has an exact convex SDP reformulation and can be solved efficiently in polynomial time.

Proposed solution. We will use the symmetrization trick to analyze the eigenvalues of $M^\top M$, but in a rather non-conventional way. Our derivation contains three steps. **Step 1:** Instead of diagonalizing $M^\top M$, we do the next-best thing: we block diagonalize M into multiple 2×2 blocks using orthonormal matrix. **Step 2:** we rewrite the objective into a polynomial of these 2×2 matrix blocks. **Step 3:** we control the eigenvalues in each block using linear matrix inequalities.

Step 1. Based on the singular value decomposition (SVD) of $A = U\Sigma V^\top = \sum_{i=1}^m \sigma_i u_i v_i^\top$, we rewrite M as follows.

$$M = \begin{bmatrix} \beta V \Sigma^\top \Sigma V^\top & V \Sigma^\top U^\top \\ -U \Sigma V^\top & 0_{m \times m} \end{bmatrix}_{(m+n) \times (m+n)} = \begin{bmatrix} \sum_{i=1}^m \beta \sigma_i^2 v_i v_i^\top & \sum_{i=1}^m \sigma_i v_i u_i^\top \\ -\sum_{i=1}^m \sigma_i u_i v_i^\top & 0_{m \times m} \end{bmatrix}_{(m+n) \times (m+n)}. \quad (26)$$

Notice that for any $i = [m]$, we have

$$\begin{bmatrix} \beta \sigma_i^2 v_i v_i^\top & \sigma_i v_i u_i^\top \\ -\sigma_i u_i v_i^\top & 0_{m \times m} \end{bmatrix}_{(m+n) \times (m+n)} = \begin{bmatrix} v_i & 0_{n \times 1} \\ 0_{m \times 1} & u_i \end{bmatrix}_{(m+n) \times 2} \begin{bmatrix} \beta \sigma_i^2 & \sigma_i \\ -\sigma_i & 0 \end{bmatrix}_{2 \times 2} \begin{bmatrix} v_i^\top & 0_{1 \times m} \\ 0_{1 \times n} & u_i^\top \end{bmatrix}_{2 \times (m+n)} \quad (27)$$

Define

$$Q_i = \begin{bmatrix} v_i & 0_{n \times 1} \\ 0_{m \times 1} & u_i \end{bmatrix} \in \mathbb{R}^{(m+n) \times 2}, \quad B(\sigma_i) = \begin{bmatrix} \beta \sigma_i^2 & \sigma_i \\ -\sigma_i & 0 \end{bmatrix} \in \mathbb{R}^{2 \times 2}. \quad (28)$$

We now block-diagonalize M using an orthonormal matrix.

$$\begin{aligned} M &= \begin{bmatrix} \sum_{i=1}^m \sigma_i^2 \beta v_i v_i^\top & \sum_{i=1}^m \sigma_i v_i u_i^\top \\ -\sum_{i=1}^m \sigma_i u_i v_i^\top & 0_{m \times m} \end{bmatrix} = \sum_{i=1}^m \begin{bmatrix} v_i & 0_{n \times 1} \\ 0_{m \times 1} & u_i \end{bmatrix} \begin{bmatrix} \beta \sigma_i^2 & \sigma_i \\ -\sigma_i & 0 \end{bmatrix} \begin{bmatrix} v_i^\top & 0_{1 \times m} \\ 0_{1 \times n} & u_i^\top \end{bmatrix} \\ &= \begin{bmatrix} Q_1 & \cdots & Q_m \end{bmatrix}_{(n+m) \times 2m} \begin{bmatrix} B(\sigma_1) & \cdots & 0 \\ & \ddots & \\ 0 & \cdots & B(\sigma_m) \end{bmatrix}_{2m \times 2m} \begin{bmatrix} Q_1^\top \\ \vdots \\ Q_m^\top \end{bmatrix}_{2m \times (n+m)} \\ &= \begin{bmatrix} Q_1 & \cdots & Q_m & \cdots & Q_{m+n} \end{bmatrix}_{(n+m) \times (n+m)} \begin{bmatrix} B(\sigma_1) & \cdots & 0 & 0 \\ & \ddots & & \\ 0 & \cdots & B(\sigma_m) & 0 \\ 0 & \cdots & 0 & 0_{(n-m) \times (n-m)} \end{bmatrix}_{(n+m) \times (n+m)} \begin{bmatrix} Q_1^\top \\ \vdots \\ Q_m^\top \\ \vdots \\ Q_{m+n}^\top \end{bmatrix}_{(n+m) \times (n+m)} \\ &:= Q \Lambda Q^\top, \end{aligned}$$

where Q_{m+1}, \dots, Q_{m+n} form the orthonormal basis of $\text{null}(M)$ and they make Q an orthonormal matrix. This property will be important for the analysis in the sequel.

Step 2. Now we rewrite (25) based on the block diagonalization of M .

$$\begin{aligned}
(25) &= \min_{\eta_1, \dots, \eta_T} \max_{A, s, t, \sigma(A) \subseteq [\mu, L], z \notin \mathcal{Z}^*} \frac{\|(I - \eta_T Q \Lambda Q^\top) \cdots (I - \eta_1 Q \Lambda Q^\top)(z - z^*)\|_2}{\|z - z^*\|_2} \\
&= \min_{\eta_1, \dots, \eta_T} \max_{A, s, t, \sigma(A) \subseteq [\mu, L], z \notin \mathcal{Z}^*} \frac{\|(I - \eta_T \Lambda) \cdots (I - \eta_1 \Lambda) Q^\top (z - z^*)\|_2}{\|Q^\top (z - z^*)\|_2} \\
&\stackrel{(a)}{=} \min_{\eta_1, \dots, \eta_T} \max_{\sigma \subseteq [\mu, L]} \|(I_{2 \times 2} - \eta_T B(\sigma)) \cdots (I_{2 \times 2} - \eta_1 B(\sigma))\|_{\text{op}} \\
&\stackrel{(b)}{=} \min_{a_1, \dots, a_T} \max_{\sigma \subseteq [\mu, L]} \left\| I_{2 \times 2} + a_1 B(\sigma) + a_2 B(\sigma)^2 \cdots + a_T B(\sigma)^T \right\|_{\text{op}}
\end{aligned}$$

where (a) is because we are maximizing over $z \notin \mathcal{Z}^*$ so we only need to consider the non-zero eigenvalues of M , which all reside in $B(\sigma)$. In (b), we rearrange the product term as a T -th order polynomial of B , and we optimize (η_1, \dots, η_T) is equivalent to optimizing the coefficient of the polynomial (a_1, \dots, a_T) .

Step 3. Note that (29) is equivalent to the formulation below.

$$\begin{aligned}
&\min_{a_1, \dots, a_T, s} \quad s \\
&\text{s.t.} \quad (I_{2 \times 2} + a_1 B(\sigma) + \cdots + a_T B(\sigma)^T)^\top (I_{2 \times 2} + a_1 B(\sigma) + \cdots + a_T B(\sigma)^T) \preceq s^2 I_{2 \times 2}, \\
&\quad \sigma \subseteq [\mu, L].
\end{aligned}$$

Note that (29) can be rewritten as follows using linear matrix inequalities:

$$\begin{aligned}
&\min_{a_1, \dots, a_T, s} \quad s \\
&\text{s.t.} \quad \begin{bmatrix} s I_{2 \times 2} & (I_{2 \times 2} + a_1 B(\sigma) + a_2 B(\sigma)^2 \cdots + a_T B(\sigma)^T)^\top \\ I_{2 \times 2} + a_1 B(\sigma) + a_2 B(\sigma)^2 \cdots + a_T B(\sigma)^T & s I_{2 \times 2} \end{bmatrix} \succeq 0, \\
&\quad \sigma \subseteq [\mu, L].
\end{aligned} \tag{29}$$

We further re-arrange it as follows:

$$\begin{aligned}
&\min_{a_1, \dots, a_T, s} \quad s \\
&\text{s.t.} \quad s I_{4 \times 4} + \begin{bmatrix} 0 & I_{2 \times 2} \\ I_{2 \times 2} & 0 \end{bmatrix}_{4 \times 4} + a_1 \begin{bmatrix} 0 & B(\sigma)^\top \\ B(\sigma) & 0 \end{bmatrix}_{4 \times 4} + \cdots + a_T \begin{bmatrix} 0 & (B(\sigma)^T)^\top \\ B(\sigma)^T & 0 \end{bmatrix}_{4 \times 4} \succeq 0, \\
&\quad \sigma \subseteq [\mu, L].
\end{aligned} \tag{30}$$

Note that (30) is an SDP, but admits an infinite number of matrix-inequality constraints. For the ease of computation, we further discretize the interval $\sigma \subseteq [\mu, L]$ by returning n_{sample} evenly spaced σ_i over $[\mu, L]$, for $i = [n_{\text{sample}}]$.

$$\begin{aligned}
&\min_{a_1, \dots, a_T, s} \quad s \\
&\text{s.t.} \quad s I_{4 \times 4} + \begin{bmatrix} 0 & I_{2 \times 2} \\ I_{2 \times 2} & 0 \end{bmatrix}_{4 \times 4} + a_1 \begin{bmatrix} 0 & B(\sigma_i)^\top \\ B(\sigma_i) & 0 \end{bmatrix}_{4 \times 4} + \cdots + a_T \begin{bmatrix} 0 & (B(\sigma_i)^T)^\top \\ B(\sigma_i)^T & 0 \end{bmatrix}_{4 \times 4} \succeq 0, \\
&\quad i = [n_{\text{sample}}].
\end{aligned} \tag{31}$$

Now Problem (31) has a finite number of constraints and only involves small-scaled matrices with size 4×4 . This problem can be efficiently solved in polynomial time using the Interior Point Methods (IPMs).

After solving (31), we factorize the polynomial $p(x) = 1 + a_1 x + a_2 x^2 \cdots + a_T x^T = (1 - \eta_1 x)(1 - \eta_2 x) \cdots (1 - \eta_T x)$ and use $\{\eta_t\}_{t=1}^T$ as the final stepsize rule. Note that the polynomial factorization process can be efficiently done via two steps: First, find the roots of $p(x)$, denoted as $\{r_t\}_{t=1}^T$. This can be efficiently done by computing the eigenvalues of the companion matrix [Horn and Johnson, 2012]. Second, take the inverse over these roots and get $\eta_t = 1/r_t$, for $t = [T]$.

The complete algorithm for finding $\{\eta_t\}_{t=1}^T$ is presented in **Algorithm 1**, and we call it Finite Horizon stepsize rule (for the primal-dual method).

3 Theoretical Guarantee for Finite Horizon Stepsize Rule

We now prove that Finite Horizon stepsize rule can reach accelerated convergence over the constant stepsize. Consider the case where is no non-negativity constraint $x \geq 0$ in (8), that is

$$\begin{aligned} \min_{x \in \mathbb{R}^n} \quad & c^\top x \\ \text{s.t.} \quad & Ax = b. \end{aligned} \quad (32)$$

To ensure the boundedness of this LP, we will assume $c \in \text{range}(A^\top)$. In this case, the objective function will be constant within the feasible set, i.e., $c^\top x = c^\top A^\top (AA^\top)^{-1}b$ for all feasible x , and the problem is equivalent to solving the linear system $Ax = b$. In this case, the primal-dual method admits the following update rule:

$$z^{t+1} - z^* = (I - \eta_t M)(z^t - z^*), \quad (33)$$

where all the variables follow the same definition in Section 2.1. We now prove that: At the T -th (pre-determined) iteration, the complexity of our stepsize rule is at most $\mathcal{O}(\sqrt{\kappa} \log(\frac{1}{\epsilon}))$, which achieves acceleration over the optimal constant stepsize $\Omega(\kappa \log(\frac{1}{\epsilon}))$, where κ is the condition number of the update matrix. We first recall the classical lower bound for the asymptotic constant step size.

Proposition 1. (Lower bound for constant stepsize) Consider problem (32) with $A \in \mathbb{R}^{m \times n}$ full row rank and $m \leq n$. Assume the singular values of A lie in $[\mu, L]$, where $\mu, L > 0$. Suppose $b \in \text{range}(A)$ and $c \in \text{range}(A^\top)$ so that (32) is feasible and bounded. Consider the primal-dual method (33) with constant stepsize. Denote $z^\top = (x^\top, y^\top) \in \mathbb{R}^{n+m}$ as the concatenation of the primal variable $x \in \mathbb{R}^n$ and dual variable $y \in \mathbb{R}^m$. Assume the augmented Lagrangian coefficient β is large such that $\beta \geq \frac{2}{\mu}$. Define the asymptotic optimal constant stepsize as:

$$\eta^* = \arg \min_{\eta} \max_{A, \text{s.t.}, \sigma(A) \subseteq [\mu, L], z \notin \mathcal{Z}^*} \limsup_{T \rightarrow \infty} \frac{\|(I - \eta M)^T(z^0 - z^*)\|_2}{\|z^0 - z^*\|_2}. \quad (34)$$

Then we have (i): $\eta^* = (\beta L^2 + \sqrt{\beta^2 L^4 - 4L^2} + \beta \mu^2 - \sqrt{\beta^2 \mu^4 - 4\mu^2})^{-1}$. (ii): For any $A, \text{s.t.}, \sigma(A) \subseteq [\mu, L]$, there exists a real-valued initialization z^0 such that the following lower bound hold at any $T > 0$:

$$\text{dist}(z^T, \mathcal{Z}^*) \geq \left(1 - \frac{2}{\frac{\beta L^2 + \sqrt{\beta^2 L^4 - 4L^2}}{\beta \mu^2 - \sqrt{\beta^2 \mu^4 - 4\mu^2}} + 1} \right)^T \text{dist}(z^0, \mathcal{Z}^*), \quad (35)$$

where $\text{dist}(z, \mathcal{Z}^*)$ denotes the Euclidean distance of z to the set of optimal primal-dual solutions. Eq. (35) can also be rewritten as follows:

$$\text{dist}(z^T, \mathcal{Z}^*) \geq \left(1 - \frac{2}{\kappa + 1} \right)^T \text{dist}(z^0, \mathcal{Z}^*), \quad (36)$$

where κ as the condition number of matrix M (as defined in (15)).

The proof can be seen in Section 4.1. This result provides a complexity lower bound $\Omega(\kappa \log(1/\epsilon))$ for the constant stepsize. Now we show that Finite Horizon stepsize rule achieves a faster convergence rate at the pre-determined T -th step.

Theorem 1. (Upper bound for Finite Horizon stepsize rule) Consider problem (32) with $A \in \mathbb{R}^{m \times n}$ full row rank and $m \leq n$. Assume the singular values of A lie in $[\mu, L]$, where $\mu, L > 0$. Suppose $b \in \text{range}(A)$ and $c \in \text{range}(A^\top)$ so that (32) is feasible and bounded. Consider the primal-dual method with Finite Horizon stepsize

rule (η_1, \dots, η_T) as in Algorithm 1. Denote $z^\top = (x^\top, y^\top) \in \mathbb{R}^{n+m}$ as the concatenation of the primal variable $x \in \mathbb{R}^n$ and dual variable $y \in \mathbb{R}^m$. Assume the augmented Lagrangian coefficient β is large such that $\beta \geq \frac{2}{\mu}$, then for any z^0 and any pre-determined T , Algorithm 1 achieves the following rate at the T -th step:

$$\text{dist}(z^T, \mathcal{Z}^*) \leq \sqrt{2 + 4\gamma} \left(1 - \frac{2}{\sqrt{\frac{\beta L^2 + \sqrt{\beta^2 L^4 - 4L^2}}{\beta \mu^2 - \sqrt{\beta^2 \mu^4 - 4\mu^2}} + 1}} \right)^T \text{dist}(z^0, \mathcal{Z}^*), \quad (37)$$

where $\gamma = 4/(\beta^2 \mu^2 - 4)$ and $\text{dist}(z, \mathcal{Z}^*)$ denotes the Euclidean distance of z to the set of optimal primal-dual solutions. Eq. (37) can also be rewritten as follows:

$$\text{dist}(z^T, \mathcal{Z}^*) \leq \sqrt{2 + 4\gamma} \left(1 - \frac{2}{\sqrt{\kappa} + 1} \right)^T \text{dist}(z^0, \mathcal{Z}^*), \quad (38)$$

where κ as the condition number of matrix M (as defined in (15)).

The proof of Theorem 1 is shown in Section 4.2. Theorem 1 provides a complexity upper bound $\mathcal{O}(\sqrt{\kappa} \log(\frac{1}{\epsilon}))$ for Finite Horizon stepsize rule at T -th step, and the upper bound achieves acceleration over the lower bound $\Omega(\kappa \log(\frac{1}{\epsilon}))$ for the constant step. It is important to note that the acceleration is reached without changing the algorithm, e.g., storing extra building blocks like momentum, and the advantage merely comes from the stepsize choice. Meanwhile, the acceleration in Theorem 1 is only guaranteed at the T -th iteration, which is fixed and finite. This is different from the classical theory that focuses on asymptotic guarantees. Our analysis is inspired by the pioneer work of GD stepsize [Young, 1953], yet we encounter new challenges raised by the non-symmetric nature of M . We provide a detailed explanation as follows.

4 Proof of Main Results

4.1 Proof of Proposition 1

The proof of Proposition 1 is just two steps. First, by Theorem 1.1 in [Young, 2014], we have (34) = $\max_{A, s.t., \sigma(A) \subseteq [\mu, L], z \notin \mathcal{Z}^*} \rho^T$ where $\rho := \max_{\lambda > 0, \lambda \in \lambda(I - \eta M)} |\lambda|$. Then, it is easy to see that $\eta^* = \frac{1}{\lambda_1 + \lambda_{2m}}$, where λ_1, λ_{2m} are the largest and smallest non-zero eigenvalues of M , respectively. Second, when initializing at $z^0 - z^* = x_{2m}$, where x_{2m} is the eigenvector of M associated with λ_{2m} , we have the following equality and this concludes the proof.

$$\text{dist}(z^T, \mathcal{Z}^*) = (1 - \eta^* \lambda_{2m})^T \text{dist}(z^0, \mathcal{Z}^*) = \left(1 - \frac{2}{\kappa + 1} \right)^T \text{dist}(z^0, \mathcal{Z}^*).$$

4.2 Proof of Theorem 1

We now prove Theorem 1. To simplify notations, we define Γ as follows. To prove Theorem 1, we need to bound the singular values of Γ .

$$\Gamma = (I - \eta_T M)(I - \eta_{T-1} M) \cdots (I - \eta_1 M). \quad (39)$$

There are at least two difficulties to prove Theorem 1 (or to bound the singular of Γ). First, M is a non-symmetric matrix, and there are not many helpful tools to bound the singular values of the product of a series of non-symmetric matrices. One potential way is to calculate the eigenvalues of $\Gamma^\top \Gamma$, but it is still not easy since M^\top and M do not commute and cannot be simultaneously diagonalized. Second, even if we explicitly calculate the singular values of Γ , they would have complicated dependency on (η_1, \dots, η_T) , and it is not clear how to relate these explicit expressions to the condition number κ of M .

The proof of Theorem 1 is summarized in the following four steps.

- **Step 1.** We explicitly calculate the eigenvalues and eigenvectors of M . This serves as the foundation of the whole proof.
- **Step 2.** We calculate the eigenvalues of $\Gamma^\top \Gamma$. The conventional way is to diagonalize $\Gamma^\top \Gamma$ using the eigenvectors of M . Although this method is useful when $M = M^\top$, we find that the diagonalization process is rather difficult when M is non-symmetric, primarily because M^\top and M cannot be simultaneously diagonalized. Here, we propose a rather unconventional way: First, we *block-diagonalize* $\Gamma^\top \Gamma$ into 2×2 blocks. Then, we calculate the eigenvalues of each block via characteristic polynomials.
- **Step 3.** We bound the eigenvalues of $\Gamma^\top \Gamma$ by the polynomial of $\lambda(M)$.
- **Step 4.** Using the optimality condition of Finite Horizon rule, we bound the polynomial of $\lambda(M)$ by the condition number κ of M . This step is done using the properties of the Chebyshev polynomial.

Step 1. We prove the following lemma to obtain the eigenvalues and eigenvectors of M . The proof of Lemma 1 can be seen in Section 4.3.

Lemma 1. Consider the update matrix of the primal-dual method M as in (15). Suppose the singular values of A are $0 < \mu \leq \sigma_m \leq \dots \leq \sigma_1 \leq L$ and suppose β is large such that $\beta \geq \frac{2}{\mu}$, then M is diagonalizable with $2m$ non-zero eigenvalues and $(n - m)$ zero eigenvalues. In particular, all $2m$ nonzero eigenvalues and the corresponding eigenvectors of M are shown as follows.

$$\lambda_{i,1}, \lambda_{i,2} = \frac{\beta\sigma_i^2 \pm \sqrt{\beta^2\sigma_i^4 - 4\sigma_i^2}}{2}, x_{i,1} = \begin{bmatrix} v_i \\ -\frac{1}{\lambda_{i,1}}Av_i \end{bmatrix}, x_{i,2} = \begin{bmatrix} v_i \\ -\frac{1}{\lambda_{i,2}}Av_i \end{bmatrix}, i = 1, \dots, m, \quad (40)$$

where v_i are the eigenvectors of $A^\top A$ associated with the nonzero eigenvalue σ_i^2 , $i = 1, \dots, m$. For the $(n - m)$ zero eigenvalues of M , the corresponding eigenvectors are

$$x_i = \begin{bmatrix} v_i \\ 0 \end{bmatrix}, i = 2m + 1, \dots, n + m, \quad (41)$$

where v_{2m+1}, \dots, v_{n+m} form the basis of $\text{null}(A^\top A)$.

Step 2. Now we explicitly calculate the eigenvalues of $\Gamma^\top \Gamma$ via block-diagonalization.

Lemma 2. Consider the matrix M and Γ as defined in (15) and (39), respectively. Denote the eigen-pairs of M using the same notations as in Lemma 1. Define $X := [x_{1,1}, \dots, x_{m,2}, x_{2m+1}, \dots, x_{n+m}] \in \mathbb{R}^{(n+m) \times (n+m)}$ as the matrix of eigenvectors of M , then we have

$$X^{-1}\Gamma^\top \Gamma X = \begin{bmatrix} B_1^2 & \dots & 0 & 0 \\ & \ddots & & \\ 0 & \dots & B_m^2 & 0 \\ 0 & \dots & 0 & I_{(n-m) \times (n-m)} \end{bmatrix}_{(n+m) \times (n+m)},$$

where $B_i := \frac{1}{\lambda_{i,1} - \lambda_{i,2}} \begin{bmatrix} \delta_{i,1}(\lambda_{i,1} + \lambda_{i,2}) & -2\delta_{i,1}\lambda_{i,2} \\ 2\delta_{i,2}\lambda_{i,1} & -\delta_{i,2}(\lambda_{i,1} + \lambda_{i,2}) \end{bmatrix} \in \mathbb{R}^{2 \times 2}$, $\delta_{i,k} = \prod_{t=1}^T (1 - \eta_t \lambda_{i,k})$, $i = [m]$, $k = [2]$.

Further, the eigenvalues of B_i^2 are

$$\begin{cases} \lambda_1(B_i^2) = \frac{1}{2} \left(\delta_{i,1}^2 + \delta_{i,2}^2 + \varepsilon_i - \sqrt{(\delta_{i,1}^2 - \delta_{i,2}^2)^2 + 2\varepsilon_i(\delta_{i,1}^2 + \delta_{i,2}^2) + \varepsilon_i^2} \right) \\ \lambda_2(B_i^2) = \frac{1}{2} \left(\delta_{i,1}^2 + \delta_{i,2}^2 + \varepsilon_i + \sqrt{(\delta_{i,1}^2 - \delta_{i,2}^2)^2 + 2\varepsilon_i(\delta_{i,1}^2 + \delta_{i,2}^2) + \varepsilon_i^2} \right), \end{cases} \quad (42)$$

where

$$\varepsilon_i = \frac{4\lambda_{i,1}\lambda_{i,2}}{(\lambda_{i,1} - \lambda_{i,2})^2} (\delta_{i,1} - \delta_{i,2})^2 = \frac{4\sigma_i^2}{\beta^2\sigma_i^4 - 4\sigma_i^2} (\delta_{i,1} - \delta_{i,2})^2 = \frac{4}{\beta^2\sigma_i^2 - 4} (\delta_{i,1} - \delta_{i,2})^2.$$

The proof of Lemma 2 is shown in Section 4.4. Note that the eigenvalues of B_i^2 in (42) are also the eigenvalues of $\Gamma^\top \Gamma$ because of the block-diagonalization.

Step 3. We now bound $\lambda(\Gamma^\top \Gamma)$ using the polynomial of $\lambda(M)$. Since $\varepsilon_i \geq 0$, we have $r_{i,1} \leq r_{i,2}$. We notice a bound

$$\varepsilon_i \leq \gamma(\delta_{i,1} - \delta_{i,2})^2 \leq 2\gamma(\delta_{i,1}^2 + \delta_{i,2}^2),$$

for some constant $\gamma = 4/(\beta^2\mu^2 - 4)$ not depending on the iteration number T . The bound implies that

$$r_{i,2} \leq \delta_{i,1}^2 + \delta_{i,2}^2 + 2\gamma(\delta_{i,1}^2 + \delta_{i,2}^2) \leq (2 + 4\gamma) \max(\delta_{i,1}^2, \delta_{i,2}^2).$$

Therefore, we have

$$\max_{\lambda \in \lambda(\Gamma^\top \Gamma), \lambda \neq 1} |\lambda|^{\frac{1}{2}} \leq \sqrt{2 + 4\gamma} \max_{i \in [2m]} (|\delta_{i,1}|, |\delta_{i,2}|) \leq \sqrt{2 + 4\gamma} \max_{\lambda \in [\lambda_{2m}, \lambda_1]} |(1 - \eta_1\lambda) \cdot (1 - \eta_2\lambda) \dots (1 - \eta_T\lambda)|. \quad (43)$$

Step 4. Finally, we bound (43) using the properties of Chebyshev polynomial. Before that, we first write down the convergence rate using the optimality condition of Finite Horizon stepsize rule in Algorithm 1.

$$\begin{aligned} \text{dist}(z^T, \mathcal{Z}^*) &\leq \max_{A, s.t., \sigma(A) \subseteq [\mu, L], z \notin \mathcal{Z}^*} \frac{\|(I - \eta_T M) \dots (I - \eta_1 M)(z - z^*)\|_2}{\|z - z^*\|_2} \text{dist}(z^0, \mathcal{Z}^*) \\ &\stackrel{\text{Algorithm 1}}{=} \min_{\eta_1, \dots, \eta_T} \max_{A, s.t., \sigma(A) \subseteq [\mu, L], z \notin \mathcal{Z}^*} \frac{\|(I - \eta_T M) \dots (I - \eta_1 M)(z - z^*)\|_2}{\|z - z^*\|_2} \text{dist}(z^0, \mathcal{Z}^*) \\ &\stackrel{(39)}{=} \min_{\eta_1, \dots, \eta_T} \max_{A, s.t., \sigma(A) \subseteq [\mu, L], z \notin \mathcal{Z}^*} \frac{\|\Gamma(z - z^*)\|_2}{\|z - z^*\|_2} \text{dist}(z^0, \mathcal{Z}^*) \\ &= \min_{\eta_1, \dots, \eta_T} \max_{A, s.t., \sigma(A) \subseteq [\mu, L], \lambda \in \lambda(\Gamma^\top \Gamma), \lambda \neq 1} |\lambda|^{\frac{1}{2}} \text{dist}(z^0, \mathcal{Z}^*) \\ &\stackrel{(43)}{\leq} \underbrace{\sqrt{2 + 4\gamma} \min_{\eta_1, \dots, \eta_T} \max_{\lambda \in [\lambda_{2m}, \lambda_1]} |(1 - \eta_1\lambda) \cdot (1 - \eta_2\lambda) \dots (1 - \eta_T\lambda)|}_{(a)} \text{dist}(z^0, \mathcal{Z}^*). \end{aligned}$$

. We denote $f_T(\lambda) = (1 - \eta_1\lambda) \cdot (1 - \eta_2\lambda) \dots (1 - \eta_T\lambda)$. We observe that $f_T(\lambda)$ is a T -th order polynomial with constraint $f_T(0) = 1$. We now bound (a) using the help of the Chebyshev polynomial [Chebyshev, 1853]. We first recall a classical proposition of the Chebyshev polynomial from the literature [Markov and Grossmann, 1916, Pedregosa, 2020], and then use it to bound (a).

Proposition 2. (Minimax polynomial) Define the linear scaling mapping $\sigma(\lambda) = \frac{\lambda_1 + \lambda_{2m}}{\lambda_1 - \lambda_{2m}} - \frac{2}{\lambda_1 - \lambda_{2m}} \lambda$, which maps the positive interval $[\lambda_{2m}, \lambda_1]$ into $[-1, 1]$. Denote the t -th order Chebyshev polynomial as $C_t(x) = \cos(t * \arccos x)$, then we have

$$\frac{C_t(\sigma(\lambda))}{C_t(\sigma(0))} = \arg \min_{f_t \in \mathcal{F}_t} \max_{\lambda \in [\lambda_{2m}, \lambda_1]} |f_t(\lambda)|, \quad s.t., f_t(0) = 1, \quad (44)$$

where \mathcal{F}_t denotes the set of t -th order polynomials.

The proof of Proposition 2 is relegated in Section 4.5. Now we bound (a) using $\frac{C_t(\sigma(\lambda))}{C_t(\sigma(0))}$.

$$\begin{aligned}
\text{dist}(z^T, \mathcal{Z}^*) &\stackrel{(43)}{\leq} \underbrace{\sqrt{2+4\gamma} \min_{\eta_1, \dots, \eta_T} \max_{\lambda \in [\lambda_{2m}, \lambda_1]} |(1-\eta_1\lambda) \cdot (1-\eta_2\lambda) \dots (1-\eta_T\lambda)|}_{(a)} \text{dist}(z^0, \mathcal{Z}^*). \\
&\stackrel{(44)}{=} \sqrt{2+4\gamma} \frac{\sup_{\lambda \in [\lambda_{2m}, \lambda_1]} |C_T(\sigma(\lambda))|}{|C_T(\sigma(0))|} \text{dist}(z^0, \mathcal{Z}^*) \tag{45} \\
&\stackrel{(a)}{=} \frac{\sqrt{2+4\gamma}}{C_T\left(\frac{\kappa+1}{\kappa-1}\right)} \text{dist}(z^0, \mathcal{Z}^*) \tag{46} \\
&\stackrel{(b)}{\leq} \frac{2\sqrt{2+4\gamma}}{\left(\frac{\kappa+1}{\kappa-1} + \sqrt{\left(\frac{\kappa+1}{\kappa-1}\right)^2 - 1}\right)^T} \text{dist}(z^0, \mathcal{Z}^*) \tag{47} \\
&\stackrel{(c)}{\leq} \sqrt{2+4\gamma} \left(\frac{\sqrt{\kappa}-1}{\sqrt{\kappa}+1}\right)^T \text{dist}(z^0, \mathcal{Z}^*) \tag{48} \\
&= \sqrt{2+4\gamma} \left(1 - \frac{2}{1+\sqrt{\kappa}}\right)^T \text{dist}(z^0, \mathcal{Z}^*), \tag{49}
\end{aligned}$$

where (a): $\sup_{x \in [-1, 1]} |C_T(x)| = 1$, $\sigma(0) = \frac{\lambda_1 + \lambda_{2m}}{\lambda_1 - \lambda_{2m}}$ and we denote $\kappa = \frac{\lambda_1}{\lambda_{2m}}$; (b): the property of Chebyshev polynomial [Pedregosa, 2020]: $C_T(x) \geq \frac{(x + \sqrt{x^2 - 1})^T}{2}$, $\forall x \notin (-1, 1)$; (c): some basic re-arrangement.

4.3 Proof of Lemma 1

We solve the following equation to get the eigenpairs of M :

$$M \begin{bmatrix} v \\ u \end{bmatrix} \stackrel{(15)}{=} \begin{bmatrix} \beta A^\top A & A^\top \\ -A & 0_{m \times m} \end{bmatrix} \begin{bmatrix} v \\ u \end{bmatrix} = \lambda \begin{bmatrix} v \\ u \end{bmatrix},$$

where $v \in \mathbb{R}^n$, $u \in \mathbb{R}^m$, and λ is an eigenvalue of M . This yields:

$$\beta A^\top A v + A^\top u = \lambda v, \tag{50}$$

$$-A v = \lambda u. \tag{51}$$

We first consider the case with $\lambda \neq 0$. From (51), we have:

$$u = -\frac{1}{\lambda} A v. \tag{52}$$

Substituting u back into equation (50), we have:

$$\beta A^\top A v - \frac{1}{\lambda} A^\top A v = \lambda v,$$

or equivalently, we have:

$$\left(\beta - \frac{1}{\lambda}\right) A^\top A v = \lambda v.$$

Since $A^\top A v = \sigma_i^2 v$ for eigenvalues σ_i^2 of $A^\top A$, we get:

$$\left(\beta - \frac{1}{\lambda}\right) \sigma_i^2 v = \lambda v.$$

This leads to the scalar equation:

$$\left(\beta - \frac{1}{\lambda}\right) \sigma_i^2 = \lambda.$$

Multiplying both sides by λ :

$$(\beta\lambda - 1)\sigma_i^2 = \lambda^2.$$

Solve this quadratic equation in λ and we will get:

$$\lambda_{i,1}, \lambda_{i,2} = \frac{\beta\sigma_i^2 \pm \sqrt{\beta^2\sigma_i^4 - 4\sigma_i^2}}{2}, i = 1, \dots, m.$$

To get the corresponding eigenvectors, we use (52) and conclude that

$$x_{i,1} = \begin{bmatrix} v_i \\ -\frac{1}{\lambda_{i,1}}Av_i \end{bmatrix}, x_{i,2} = \begin{bmatrix} v_i \\ -\frac{1}{\lambda_{i,2}}Av_i \end{bmatrix}, i = 1, \dots, m.$$

We now calculate the eigenvectors corresponding to 0 eigenvalues. In this case, we have $Au = 0$ from (51). Plugging it into (50) and we have

$$A^\top u = 0.$$

Since $A \in \mathbb{R}^{m \times n}$ is full row rank with $m < n$, we have $u = 0$. Therefore, the eigenvectors for the zero eigenvalues are

$$x_i = \begin{bmatrix} v_i \\ 0 \end{bmatrix}, i = 2m+1, \dots, n+m,$$

where v_{2m+1}, \dots, v_{n+m} form the basis of $\text{null}(A)$, or equivalently, the basis of $\text{null}(A^\top A)$. Finally, we note that all these eigenvectors $x_{i,1}, x_{i,2}, i = 1, \dots, m$ and x_{2m+1}, \dots, x_{n+m} are linearly independent, so M is diagonalizable.

4.4 Proof of Lemma 2

We define the matrix Ω as:

$$\Omega = \begin{bmatrix} I_{n \times n} & 0 \\ 0 & -I_{m \times m} \end{bmatrix}.$$

Note that Ω is involutive ($\Omega^2 = I$) and symmetric ($\Omega^\top = \Omega$), and it is easy to see that $M^\top = \Omega M \Omega$. Now we investigate how Ω affects the eigenvectors of M . Let $x_{i,1}, x_{i,2}$ be eigenvectors of M corresponding to eigenvalues $\lambda_{i,1}, \lambda_{i,2}$ as defined in (40). Applying Ω to $x_{i,1}, x_{i,2}$ and we get:

$$\Omega x_{i,k} = \begin{bmatrix} v_i \\ \frac{1}{\lambda_{i,k}}Av_i \end{bmatrix}, k = 1, 2.$$

Let us express $\Omega x_{i,k}$ in terms of $x_{i,1}$ and $x_{i,2}$. We can write:

$$\begin{aligned} \Omega x_{i,1} &= \begin{bmatrix} v_i \\ \frac{1}{\lambda_{i,1}}Av_i \end{bmatrix} = c_{i,1} \begin{bmatrix} v_i \\ -\frac{1}{\lambda_{i,1}}Av_i \end{bmatrix} + c_{i,2} \begin{bmatrix} v_i \\ -\frac{1}{\lambda_{i,2}}Av_i \end{bmatrix} = c_{i,1}x_{i,1} + c_{i,2}x_{i,2} \\ \Omega x_{i,2} &= \begin{bmatrix} v_i \\ \frac{1}{\lambda_{i,2}}Av_i \end{bmatrix} = d_{i,1} \begin{bmatrix} v_i \\ -\frac{1}{\lambda_{i,1}}Av_i \end{bmatrix} + d_{i,2} \begin{bmatrix} v_i \\ -\frac{1}{\lambda_{i,2}}Av_i \end{bmatrix} = d_{i,1}x_{i,1} + d_{i,2}x_{i,2} \end{aligned}$$

We determine the coefficients $c_{i,1}, c_{i,2}$ and $d_{i,1}, d_{i,2}$ by solving these equations. The results are shown below.

$$\begin{bmatrix} c_{i,1} & c_{i,2} \\ d_{i,1} & d_{i,2} \end{bmatrix} = \frac{1}{\lambda_{i,1} - \lambda_{i,2}} \begin{bmatrix} \lambda_{i,1} + \lambda_{i,2} & -2\lambda_{i,2} \\ 2\lambda_{i,1} & -(\lambda_{i,1} + \lambda_{i,2}) \end{bmatrix} \quad (53)$$

Since $x_{i,k}$ is the eigenvectors of M associated with eigenvalue $\lambda_{i,k}$, we have

$$\Gamma x_{i,k} = \prod_{t=1}^T (1 - \eta_t \lambda_{i,k}) x_{i,k}.$$

Denote $\delta_{i,k} = \prod_{l=1}^T (1 - \eta_l \lambda_{i,k})$. Using the coefficients in (53), we can express $\Omega\Gamma x_{i,k}$ in terms of $x_{i,k}$, $k = 1, 2$.

$$\begin{aligned}\Omega\Gamma x_{i,1} &= \delta_{i,1} \begin{bmatrix} v_i \\ \frac{1}{\lambda_{i,1}} Av_i \end{bmatrix} = \delta_{i,1} c_{i,1} \begin{bmatrix} v_i \\ -\frac{1}{\lambda_{i,1}} Av_i \end{bmatrix} + \delta_{i,1} c_{i,2} \begin{bmatrix} v_i \\ -\frac{1}{\lambda_{i,2}} Av_i \end{bmatrix} = \delta_{i,1} c_{i,1} x_{i,1} + \delta_{i,1} c_{i,2} x_{i,2}. \\ \Omega\Gamma x_{i,2} &= \delta_{i,2} \begin{bmatrix} v_i \\ \frac{1}{\lambda_{i,2}} Av_i \end{bmatrix} = \delta_{i,2} d_{i,1} \begin{bmatrix} v_i \\ -\frac{1}{\lambda_{i,1}} Av_i \end{bmatrix} + \delta_{i,2} d_{i,2} \begin{bmatrix} v_i \\ -\frac{1}{\lambda_{i,2}} Av_i \end{bmatrix} = \delta_{i,2} d_{i,1} x_{i,1} + \delta_{i,2} d_{i,2} x_{i,2}.\end{aligned}$$

Define $B_i := \frac{1}{\lambda_{i,1} - \lambda_{i,2}} \begin{bmatrix} \delta_{i,1}(\lambda_{i,1} + \lambda_{i,2}) & -2\delta_{i,1}\lambda_{i,2} \\ 2\delta_{i,2}\lambda_{i,1} & -\delta_{i,2}(\lambda_{i,1} + \lambda_{i,2}) \end{bmatrix} \in \mathbb{R}^{2 \times 2}$, $i = [m]$, and $X := [x_1, \dots, x_{n+m}] \in \mathbb{R}^{(n+m) \times (n+m)}$. We have

$$\Omega\Gamma X = X \begin{bmatrix} B_1 & \cdots & 0 & 0 \\ & \ddots & & \\ 0 & \cdots & B_m & 0 \\ 0 & \cdots & 0 & I_{(n-m) \times (n-m)} \end{bmatrix}_{(n+m) \times (n+m)}.$$

Therefore, we have

$$X^{-1}\Gamma^\top\Gamma X = X^{-1}\Omega\Gamma\Omega\Gamma X = \begin{bmatrix} B_1^2 & \cdots & 0 & 0 \\ & \ddots & & \\ 0 & \cdots & B_m^2 & 0 \\ 0 & \cdots & 0 & I_{(n-m) \times (n-m)} \end{bmatrix}_{(n+m) \times (n+m)}.$$

To bound the largest non-one eigenvalue of $\Gamma^\top\Gamma$, we need to calculate the eigenvalues of B_i^2 and find the largest one. We calculate the roots of the characteristic polynomial of B_i^2 and we get:

$$\begin{cases} \lambda_1(B_i^2) = \frac{1}{2} \left(\delta_{i,1}^2 + \delta_{i,2}^2 + \varepsilon_i - \sqrt{(\delta_{i,1}^2 - \delta_{i,2}^2)^2 + 2\varepsilon_i(\delta_{i,1}^2 + \delta_{i,2}^2) + \varepsilon_i^2} \right) \\ \lambda_2(B_i^2) = \frac{1}{2} \left(\delta_{i,1}^2 + \delta_{i,2}^2 + \varepsilon_i + \sqrt{(\delta_{i,1}^2 - \delta_{i,2}^2)^2 + 2\varepsilon_i(\delta_{i,1}^2 + \delta_{i,2}^2) + \varepsilon_i^2} \right), \end{cases}$$

where

$$\varepsilon_i = \frac{4\lambda_{i,1}\lambda_{i,2}}{(\lambda_{i,1} - \lambda_{i,2})^2} (\delta_{i,1} - \delta_{i,2})^2 = \frac{4\sigma_i^2}{\beta^2\sigma_i^4 - 4\sigma_i^2} (\delta_{i,1} - \delta_{i,2})^2 = \frac{4}{\beta^2\sigma_i^2 - 4} (\delta_{i,1} - \delta_{i,2})^2.$$

4.5 Proof of Proposition 2

Proposition 2 is classical results of Chebyshev polynomial [Markov and Grossmann, 1916, Pedregosa, 2020]. For completeness of the whole proof, we restate the proof of this classical result under our notations. To prove Proposition 2, we need to first prove the following Proposition 3.

Proposition 3. (Equioscillation) *Consider the t -th order Chebyshev polynomial $C_t(x) = \cos(t * \arccos x)$, then for $x \in [-1, 1]$, there exists $x_0 < x_1 < \dots < x_t \in [-1, 1]$, s.t. $C_t(x_k) = (-1)^k$, $k = 0, \dots, n$. In other words, $T_t(x)$ has $(t + 1)$ extreme points in $x \in [-1, 1]$.*

The proof of Proposition 3 is just one line: for any $k = 0, 1, \dots, t$, define $x_k = \cos\left(\frac{k\pi}{t}\right)$, then we have the following equation and conclude the proof.

$$C_t(x_k) = \cos\left(t * \arccos\left(\cos\left(\frac{k\pi}{t}\right)\right)\right) = \cos(k\pi) = (-1)^k.$$

We now prove Proposition 2 by contradiction. We will show that if the problem (44) has a better solution, then that solution must at least be a $(t + 1)$ -th degree polynomial.

Since $\sigma(\lambda)$ is a linear translation from $[\lambda_{2m}, \lambda_1]$ into $[-1, 1]$, $\frac{C_t(\sigma(\lambda))}{C_t(\sigma(0))}$ has $(t + 1)$ extreme points on $[\lambda_{2m}, \lambda_1]$. By the Equioscillation property of Chebyshev polynomial (Proposition 3), the image at these extreme points have the same absolute values and they are alternately positive and negative. Now suppose there exists t -th order polynomial $R_t(\lambda)$, s.t.: $R_t(0) = 1$ but $R_t(\lambda)$ has smaller maximum absolute value. Consider $Q(\lambda) \stackrel{\text{def}}{=} \frac{C_t(\sigma(\lambda))}{C_t(\sigma(0))} - R_t(\lambda)$, $Q(\lambda)$ still alternately > 0 or < 0 at all $(t + 1)$ extreme points, so Q must have t zeros in $[\lambda_{2m}, \lambda_1]$. However, $Q(0) = P_t(0) - R_t(0) = 0$, so Q has $(t + 1)$ zeros. This forms a Contradiction. Therefore, $\frac{C_t(\sigma(\lambda))}{C_t(\sigma(0))}$ is the optimal solution to the constrained minimax problem (44).

5 Experiments

Now we verify the effectiveness of Finite Horizon stepsize rule (Algorithm 1) of the primal-dual method on various LP instances. All experiments are conducted on Intel(R) Xeon(R) Gold 6226 CPU @ 2.70GHz with 48 cores.

Setups. For all experiments, we choose $\beta = 4/\mu$, where μ is the smallest non-zero singular value of A . This choice of β satisfies the condition in Theorem 1. To solve the SDP sub-problem in Algorithm 1, we use SCS solver in cvxpy library⁴ with the configuration $n_{\text{sample}} = 200$, $\text{alpha} = 1.5$, and $\text{sdp_iter} = 100$ (the number of iterations of SDP solver to solve (31)). We set this configuration as the default choice and will not change it unless mentioned otherwise. For all experiments, we use Gaussian random initialization $\mathcal{N}(5, 1)$ to initialize the primal and dual variables. We choose the mean value of Gaussian to be 5 to keep the primal variable away from the origin and thus reduce the possibility of the projection. We define the optimality gap as the relative KKT residue [Xiong and Freund, 2023], i.e., the sum of primal feasibility, dual feasibility, and primal-dual gap, in the relative sense: $\epsilon(x, y) := \frac{\|Ax^+ - b\|}{1 + \|b\|} + \frac{\|(c - A^T y)^-\|}{1 + \|c\|} + \frac{|c^T x^+ - b^T y|}{1 + |c^T x^+| + |b^T y|}$.

5.1 Case Study on the Toy Example: Intuition and Initial Results

We first focus on a simple LP to gain intuition and boost understanding of Finite Horizon stepsize rule. We consider $c = A = 1, b = 200$, i.e.:

$$\begin{aligned} \min_{x \in \mathbb{R}^n} \quad & x \\ \text{s.t.} \quad & x = 200 \\ & x \geq 0. \end{aligned} \tag{54}$$

For this example, we have $M = \begin{bmatrix} \beta & 1 \\ -1 & 0 \end{bmatrix} = \begin{bmatrix} 4 & 1 \\ -1 & 0 \end{bmatrix}$ under the choice of $\beta = \frac{4}{\mu} = 4$. The optimal primal-dual solution is $(x^*, y^*) = (200, 1)$. We consider two versions of optimal constant stepsize rules as the baseline methods.

Baseline method 1: T -step optimal constant stepsize. We consider the optimal constant stepsize within T total iterations, i.e.,

$$\min_{\eta} \max_{A, s.t., \sigma(A) \subseteq [\mu, L]} \|(I - \eta M)^T\|_{\text{op}}. \tag{55}$$

Since $A = 1 \in \mathbb{R}$ in this toy example, the interval of $\sigma(A)$ degenerates into a single point $\mu = L = 1$ and the above minimax problem (55) reduces to the following problem.

$$\min_{\eta} \|(I - \eta M)^T\|_{\text{op}}. \tag{56}$$

⁴<https://www.cvxgrp.org/scs/>

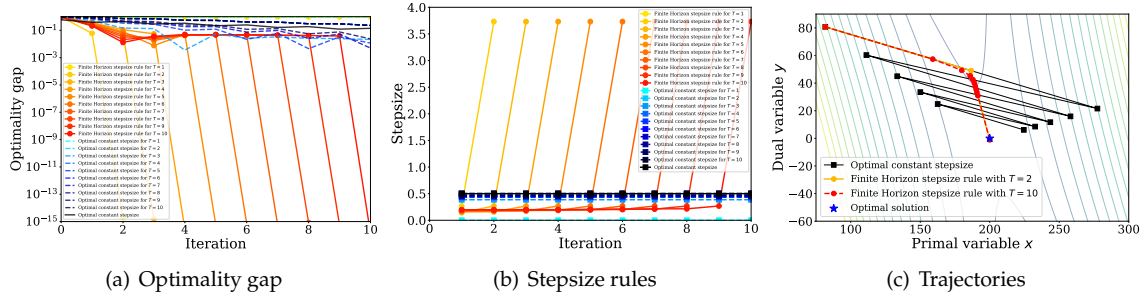


Figure 3: Results on the toy LP instance (54). For Finite Horizon stepsize rule, we find that (a): the optimality gap will drop sharply at the T -th step; (b) there will be a sudden surge at the T -th step; (c): the iterates by Finite Horizon stepsize rules will take smaller steps in the sharp region, and then take large steps in the flat region.

Problem (56) is a 1-dimensional (nonconvex) optimization problem. It can be solved to near-global optimal solution using Stimulated Annealing methods [Tsallis, 1988, Xiang et al., 2013]. In this work, we use the algorithm described in [Xiang et al., 2013] and use the implementation in `scipy` library⁵.

Note that when $T = 1$, (55) reduces to Finite Horizon stepsize rule for $T = 1$. We will see that the annealing methods to produce the same results as the SDP solver for (31) in this case.

Baseline method 2: ∞ -step optimal constant stepsize. We consider the asymptotic optimal constant stepsize when $T \rightarrow \infty$.

$$\begin{aligned}
 & \min_{\eta} \max_{A, s.t., \sigma(A) \subseteq [\mu, L]} \lim_{T \rightarrow \infty} \|(I - \eta M)^T\|_{\text{op}}^{\frac{1}{T}}. \\
 \stackrel{(a)}{=} & \min_{\eta} \max_{A, s.t., \sigma(A) \subseteq [\mu, L]} \rho(I - \eta M) \\
 \stackrel{(b)}{=} & \frac{2}{\lambda_1 + \lambda_{2m}}, \tag{57}
 \end{aligned}$$

where λ_1 and λ_{2m} are the largest and smallest non-zero eigenvalues of M . (a) is due to the property of spectral radius $\rho(A) = \lim_{T \rightarrow \infty} \|A^T\|_{\text{op}}^{\frac{1}{T}}$ [Saad, 2003, Theorem 1.12]. (b) relies on two properties of M : When the augmented Lagrangian coefficient satisfies $\beta \geq \frac{2}{\mu}$, we have: (i) M is diagonalizable. (ii) all eigenvalues of M are real-valued. Further, λ_1 and λ_{2m} can both be calculated using the extreme singular values of A , i.e., μ and L . We present their relation as below:

$$\begin{cases} \lambda_1 = \frac{\beta L^2}{2} + \sqrt{\frac{\beta^2 L^4}{4} - L^2} \stackrel{(*)}{=} \frac{2L^2}{\mu} + \sqrt{\frac{4L^4}{\mu^2} - L^2} \\ \lambda_{2m} = \frac{\beta L^2}{2} - \sqrt{\frac{\beta^2 L^4}{4} - L^2} \stackrel{(*)}{=} \frac{2L^2}{\mu} - \sqrt{\frac{4L^4}{\mu^2} - L^2}, \end{cases} \tag{58}$$

(*) holds under our default choice of $\beta = \frac{4}{\mu}$. Detailed derivation and proof can be seen in the proof of Lemma 1. In the experiments, we refer to Baseline method 1 as “optimal constant stepsize for $T = t$ ” and refer Baseline method 2 as “optimal constant stepsize”.

Remark 1: if M is symmetric, then Baseline method 1 and 2 are the same and both equal to $\eta^* = \frac{2}{\lambda_1 + \lambda_{n+m}}$. However, for non-symmetric M , these two baseline methods are different (see Figure 3). This is because

⁵https://docs.scipy.org/doc/scipy/reference/generated/scipy.optimize.dual_annealing.html

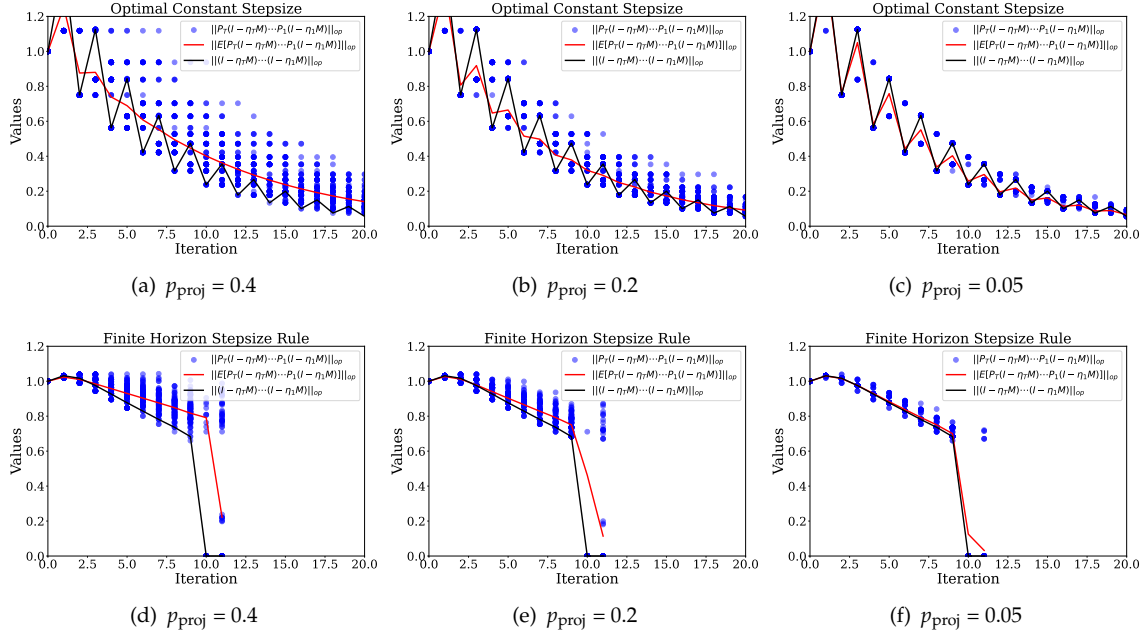


Figure 4: The evolution spectral norm of three types of error matrices along iterations. We use the total iteration budget $T = 10$ for Finite Horizon stepsize rule. We find that: the expected error matrix under projection (red curve) is close to that of the error matrix without projection (black curve), and their similarity grows when the projection probability p_{proj} shrinks to 0. Further, Finite Horizon stepsize rule can help the black curve reach almost zero error at the final step ($T = 10$), while the optimal constant stepsize cannot.

Baseline method 1 controls singular values, while Baseline method 2 controls eigenvalues. For non-symmetric matrices, these two are usually different (see discussion in Section 2).

Remark 2: Same information queried from LP class. We emphasize that both methods query the same amount of problem information to determine the hyperparameters: they both query the largest & smallest singular values of A , i.e., μ and L . However, they use this information in a different way. For the optimal constant stepsize, it uses μ and L to calculate stepsize using the formulas in (58). For Finite Horizon stepsize rule, it uses μ and L to solve the SDP sub-problem (31). In the following, we will show that Finite Horizon stepsize rule consistently outperforms the optimal constant stepsize.

Results on the toy example (54). In Figure 3, we run the primal-dual method with Finite Horizon stepsize rule for $T \leq 10$ and compare them to the corresponding optimal constant stepsize counterparts. We find that: for Finite Horizon stepsize rule with the total iteration budget T , the first $(T - 1)$ -th stepsizes will be smaller than the optimal constant step size, and then there will be a sudden surge at the T -th step. Accordingly, the optimality gap decays similarly to that of the constant step size for the first $(T - 1)$ -th steps, but it will drop sharply at the T -th step and reach the optimal primal-dual solution. This aligns with our theoretical predictions: Finite Horizon stepsize rule is designed to reach a fast convergence rate at T -th step, and there is no acceleration guarantee for steps before T . In Figure 3 (c), we see that the iterates by Finite Horizon stepsize rules will take smaller steps in the sharp region, and then take large steps in the flat region.

Spectral norm investigation. We further investigate the changes of error matrices along iterations. For Finite Horizon stepsize rule, we set the total iteration budget to be $T = 10$. For each iteration t , we compare the spectral norm of three types of error matrices:

- (i) The error matrix with projection: $P_t(I - \eta_t M) \cdots P_1(I - \eta_1 M)$, where P_1, \dots, P_t are random projection matrices as defined in (21). For each iteration t , we randomly generate 100 samples of P_t .
- (ii) The expected error matrix with projection: $\mathbb{E} [P_t(I - \eta_t M) \cdots P_1(I - \eta_1 M)]$.
- (iii) The error matrix without projection: $(I - \eta_t M) \cdots (I - \eta_1 M)$.

The results are shown in Figure 4. We find that the spectral norm of the expected error matrix (red curve) is close to that of the error matrix without projection (black curve). Further, their similarity grows when the projection probability p_{proj} shrinks to 0. This phenomenon indicates that: if the p_{proj} is small, we can effectively control the expected error rate (red curve) by manipulating the spectral norm of the error matrix without projection $\|(I - \eta_t M) \cdots (I - \eta_1 M)\|_{\text{op}}$ (black curve). As such, the SDP formulation of Finite Horizon stepsize rule (31), which focuses on optimizing the decay rate of the black curve, can provide good choices on stepsize rules. Indeed, the black curve reaches 0 error at $T = 10$ (see Figure 4 (d,e,f)), while optimal constant stepsize cannot make it. In the sequel, we will verify that p_{proj} is indeed small on real-world LP instances, and Finite Horizon stepsize rule is effective.

5.2 Results on Real-World LP Instances

Now we verify the effectiveness of Finite Horizon stepsize rule on real-world LP instances.

Setups. We consider Netlib LP benchmark [Gay, 1985] more than 90 real-world LP instances⁶. The largest instance has $m = 6084$ constraints and $n = 12243$ variables. We set the stopping criteria as follows: for some easy instances, we set the targeted error as $\epsilon(x, y) = 1e-4$; for other hard instances, we set the targeted error as $\epsilon(x, y) = 1e-1$ with an algorithm termination condition after $1e5$ iterations. If the constant stepsize method hits the termination condition after $1e5$ iterations, we will stop Finite Horizon method when it reaches the final precision of the constant stepsize method. For Finite Horizon stepsize rule, we set the total iteration budget $T \leq 10$. For those with $T = 10$, we adjust `sdp_iter` (the number of iterations of SDP solver to solve (31)) from 100 to 20 and find that it is sufficient to bring good performance. We did not use larger T since we find that further increasing T will slow down the SDP solver for solving the sub-problem (31), and the SDP solver will encounter numerical instability due to the high-degree matrix polynomial constraints. If the algorithm does not reach the desired precision after T steps, we will apply Finite Horizon stepsize strategy in a cyclical manner until the stopping criteria are met. We find that **“cyclically repeating the stepsize rule” is an effective trick** to extend Finite Horizon stepsize rule with small T to the large- T scenarios.

We compare Finite Horizon stepsize rule to the optimal constant stepsize (Baseline 2), i.e., $\eta^* = 2/(\lambda_1 + \lambda_{2m})$, where λ_1 and λ_{2m} are expressed in (58). Here, we did not consider T -step optimal constant stepsize (Baseline 1) since it is unclear how to solve the minimax problem (55).

As mentioned above, both Finite Horizon stepsize rule and the optimal constant stepsize query the same problem information to determine the hyperparameters: they both query the largest & smallest singular values of A , i.e., μ and L , but this information is used differently and results in different stepsize rules.

Case Study on Netlib-AGG Instance. We first provide a case study on Netlib-AGG with $m = 488$ $n = 615$. We conduct Finite Horizon stepsize rule for $T = 1, 2, \dots, 10$ and compare them to the optimal constant stepsize. The results are shown in Figure 5. Similarly to the observations on the toy example (Section 5.1), the stepsize will increase sharply at the T -th step and will result in a significant decrease in the optimality gap.

We also observe some different phenomena from the previous toy example. In the previous toy example, the final stepsize was the same for different T (see Figure 5 (b)), whereas here, larger T results in larger final stepsize. Accordingly, the optimality gap will decrease to a smaller value. The reason for this difference is that in the previous toy example, the optimal value is already reached at the T -th step, whereas it has not been reached here.

⁶https://github.com/scipy/scipy/tree/main/benchmarks/benchmarks/linprog_benchmark_files

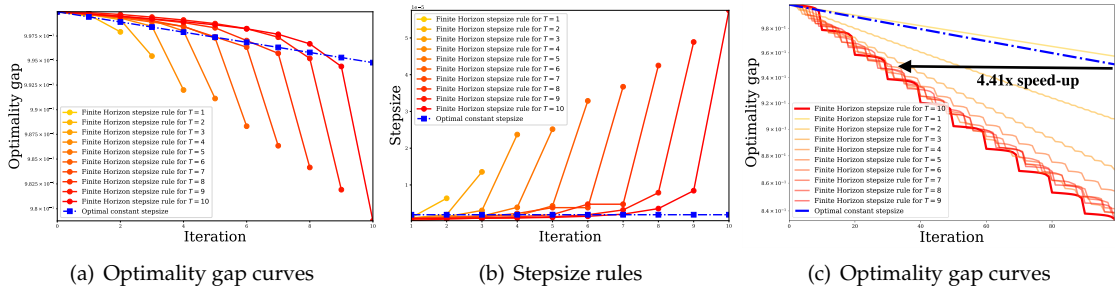


Figure 5: An example of Finite Horizon stepsize rule on real-world LP instance (NetLib-AGG). We find: (a, b) for Finite Horizon stepsize rule, the optimality gap will decrease significantly at the T -th step. Meanwhile, the stepsize will increase sharply; (c) Finite Horizon stepsize rule for $T > 1$ consistently outperforms optimal constant stepsize.

In Figure 5 (c), we further run the algorithm for 100 iterations by cyclically repeating the stepsize rule. We find that Finite Horizon stepsize rule for $T > 1$ consistently outperforms the optimal constant stepsize and $T = 10$ performs the best. We observe $4.41 \times$ speed-up in this case. For the rest of the instances in NetLib benchmark, we will choose $T = 10$ and omit the others.

Figure 6 shows the projection ratio (i.e., the proportion of entries in x that are forced to 0) along iterations on NetLib-AGG. We find that the ratio is consistently small ($< 5\%$) along the trajectories. More specifically, the average projection ratio is 4.3% and 4.7% for the constant and Finite Horizon stepsize rule, respectively. This supports the assumption on small p_{proj} in Section 2.

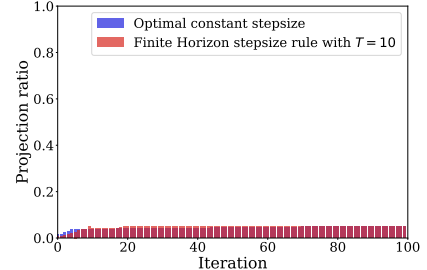


Figure 6: The projection ratio (i.e., the proportion of entries in x that are forced to 0) along iterations is consistently small ($< 5\%$).

More Results on NetLib Benchmark. We now demonstrate more results on NetLib benchmark. Figure 7 (a) demonstrates Finite Horizon stepsize rule for $T = 10$ on all the instances in NetLib Benchmark. We demonstrate the results up to 30 iterations with 3 repeated cycles of the stepsize rules. We observe a universal pattern across all LP instances: the stepsize at the final iteration ($T = 10$) increases sharply, and the magnitude of this increase depends on the specific instance. Interestingly, this pattern is similar to the recent stepsize rules for GD, where a large stepsize will appear once in a while among several small ones (e.g., [Altschuler and Parrilo, 2023]). We leave more investigation on this pattern as a future direction.

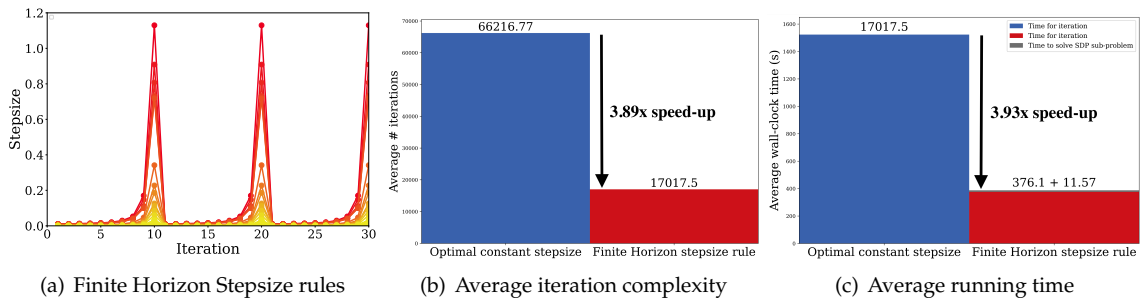


Figure 7: **(a):** Finite Horizon stepsize rule for $T = 10$ on all the instances in NetLib. We observe that the stepsize at the final iteration ($T = 10$) always increases sharply. **(b,c):** Average iteration complexity and running time to on NetLib. Our stepsize rule achieves on average $3.89 \times$ and $3.93 \times$ speed-up in terms of the number of iterations and wall-clock time, respectively. Further, the SDP sub-problem takes negligible time to solve (11.57 seconds, $< 3.1\%$ of total time).

Figure 7 (b,c) reports the average speed-up of Finite Horizon stepsize rule over the optimal constant stepsize to hit the same stopping criteria. The results are averaged over all the LP instances from NetLib

benchmark. In Table 1, we also present a detailed running time analysis for the top-10 largest instances from Netlib. We summarize the key observations here. In terms of iteration complexity, our stepsize rule saves **74.30%** iterations over the optimal constant stepsize to reach the same precision, which achieves on average **3.89 \times** speed-up. In terms of running time, our stepsize rule saves **75.31%** wall-clock time, which achieves **3.93 \times** speed-up. Further, the SDP sub-problem takes an average 11.57 seconds to solve, which is negligible compared to the overall running time (3.1 %). Note that the time for solving the SDP sub-problem does not increase with the problem size, since the SDP sub-problem only involves matrices sized 4×4 .

Nevertheless, we acknowledge that the 11.57 seconds might still be too expensive for scenarios with millisecond-level time budgets. We believe there is significant room for improvement in both the design and implementation of this approach, which we leave for future work.

Table 1: The wall-clock running time (s) for different methods on the 10 largest datasets in the Netlib Benchmark. Note that the time for solving the SDP sub-problem does not increase with the problem size, since the SDP sub-problem only involves matrices sized 4×4 .

Dataset	# constraints	# variables	Time for constant stepsize (s) / # iterations	Time for Finite Horizon stepsize rule		Total time (speed-up ratio)
				Time to solve SDP (s)	Time for iteration (s) / # iterations	
DFL001	6084	12243	983.91 / 2903	7.28	231.12 / 661	238.40 (75.77 % ↓)
QAPI2	3192	8856	4527.73 / 12986	15.60	864.66 / 2199	880.26 (80.56 % ↓)
PILOT	2875	6294	17751.92 / 100001	8.37	6314.68 / 33931	6323.05 (64.38 % ↓)
SIERRA	3263	4771	21426.60 / 22274	7.25	1860.69 / 33931	1867.94 (91.28 % ↓)
D2Q06C	2171	5831	11174.35 / 22630	10.67	5026.00 / 33931	5036.66 (54.93 % ↓)
BNL2	2324	4486	7571.56 / 54761	9.68	1354.14 / 12391	1363.82 (81.99 % ↓)
WOODW	1098	8418	6853.10 / 21540	9.36	1538.90 / 12391	1548.26 (77.41 % ↓)
CYCLE	1980	3448	6265.64 / 22637	9.23	1396.78 / 12391	1406.02 (77.56 % ↓)
STOCFOR2	2157	3045	3381.69 / 22630	10.18	712.24 / 12391	722.42 (78.64 % ↓)
SHIP12L	1151	5533	3567.07 / 22590	8.14	1153.50 / 12391	1161.64 (67.43 % ↓)

6 Related Works

In addition to all the related works described above, we now mention more literature on the stepsize design of GD, performance estimation of first-order methods, and algorithms for solving LP.

Stepsize design of GD. There is extensive research on designing stepsize rules for vanilla GD for unconstrained minimization problems. The most simple and classical textbook stepsize choice of GD is the constant stepsize, which has guarantees on generic smooth functions [Nesterov et al., 2018]. There are also some classical adaptive strategies including exact line search [Boyd and Vandenberghe, 2004], Armijo-Goldstein rule [Nesterov et al., 2018], Barzilai-Borwein-type stepsize [Barzilai and Borwein, 1988], Polyak-type stepsize [Pedregal, 2004], etc.. However, these adaptive stepsize strategies either have limited theoretical justification for their benefits, or are already known to have no improvement over constant stepsize in the worst case [De Klerk et al., 2017, Li and Sun, 2021].

The very first theoretical justification for the time-varying stepsize is from the pioneer work [Young, 1953]. For unconstrained quadratic minimization, Young [1953] showed in 1953 that GD can be accelerated using non-constant stepsizes, if the total iteration T is pre-determined (as in the finite horizon setup). The stepsize rule is given explicitly as the inverses of the roots of Chebyshev polynomials, and we will refer to it as Young’s stepsize. The results in [Young, 1953], for the very first time, revealed that time-varying stepsizes can perform better than constant ones. However, Young’s stepsize highly relies on the special connection between quadratic minimization and minimax polynomial theory, and no analysis has yet succeeded in extending it to non-quadratic cases over the past 70 years. Young’s stepsize was recently confirmed to be “not generalizable beyond quadratic” by [Altschuler, 2018, Chapter 8], where the authors showed that it is provably bad for generic convex settings. For decades, researchers have shifted their attention to other designs, such as adding extra building blocks beyond choosing stepsizes, e.g., via momentum [Nesterov, 1983]. There has been limited progress on the stepsize design of GD since [Young, 1953].

A recent influential work [Altschuler, 2018] has once again brought people’s attention back to stepsize design of GD. Perhaps a bit surprisingly, the authors proposed a new stepsize rule of vanilla GD that can bring acceleration beyond quadratic problems. Since then, a series of new stepsize design has emerged. These designs have theoretical benefits under different settings. To better put them into our context, we here only highlight their dependency on the iteration horizon T . [Altschuler, 2018] provided an optimal stepsize for $T = 2, 3$ for strongly convex functions. By cycling through these stepsizes, a constant factor improvement is achieved over the standard unaccelerated rate for constant stepsizes. For the non-strongly-convex setting, other stepsize rules of GD are developed under different iteration horizons including $T = 2, 3$ [Daccache et al., 2019], $T = 25$ [Das Gupta et al., 2024], and $T = 127$ [Grimmer, 2024]. Recently, [Altschuler and Parrilo, 2023, 2024] proposed the silver stepsize schedules that can achieve acceleration for $T = 2^k - 1$ for arbitrary $k \in \mathbb{N}_+$. The convergence rate was later refined by a factor of 2 in [Wang et al., 2024] under the same requirement of T , and has been extended to proximal gradient very recently [Bok and Altschuler, 2024]. Concurrent to the silver stepsize schedule, [Grimmer et al., 2023, 2024a] also uncovered a new stepsize schedule that brings acceleration at $T = 2^k - 1$ for arbitrary $k \in \mathbb{N}_+$. Inspired by the aforementioned works, Zhang and Jiang [2024], Grimmer et al. [2024b] further proposed to construct new stepsize schedules by concatenating shorter ones, and Zhang and Jiang [2024] proved accelerated rate for any pre-determined T (as in the finite horizon setup). Zhang et al. [2024] further carefully removed the dependency of T from the stepsize construction and established “anytime accelerated convergence” over the constant stepsize (albeit at a slower rate than that of the silver stepsize schedule [Altschuler and Parrilo, 2023, 2024]). The results in [Zhang et al., 2024] answered the open question posted in [Kornowski and Shamir, 2024]. There are also new conjectures and insights into the behaviors of constant-stepsize GD [Eloi and Glineur, 2022, Grimmer et al., 2024c, Rotaru et al., 2024].

The above works focus on theoretical acceleration. In deep learning field, there are also many new stepsize (learning rate) designs targeted for better empirical performance, e.g., ReduceLROnPlateau [Sun, 2020]⁷, warm-up [He et al., 2016, Goyal et al., 2017], cyclic learning rate [Smith, 2017, Fu et al., 2019], Cosine Annealing [Loshchilov and Hutter, 2016], and many other recent proposals [Defazio et al., 2023, Ibrahim et al., 2024, Hu et al., 2024, Defazio et al., 2024]. Some of these stepsize schedules are theoretically studied in some special function classes such as river valley landscape [Wen et al., 2024], and objectives with structured Hessian spectrum (e.g., two-cluster [Oymak, 2021, Goujaud et al., 2022] and multiscale [Kelner et al., 2022]). The interplay between stepsize choice and logistic loss is also studied in [Wu et al., 2024, Cai et al., 2024].

We now summarize the difference between our work and the works above. These works primarily focus on GD for unconstrained minimization⁸, while we study the primal-dual method for LP. One fundamental difference between these two settings is that: for the primal-dual method, its update matrix is non-symmetric (i.e., M is non-symmetric in (32)), whereas for GD, its update matrix (Hessian) is always symmetric. We highlight that non-symmetric update matrix will raise discrepancies between its singular values and eigenvalues, which do *not* exist in the symmetric case. We find that such discrepancies will substantially changes the principle for the time-varying stepsize design, especially in the *non-asymptotic* case when T is bounded. More detailed discussions on the technical challenges can be seen in Section 2.

Performance estimation problem (PEP) for first-order methods. Parallel to the aforementioned works on GD, there is an active line of works analyzing the worst-case performance of a given first-order method (including but not limited to GD) for unconstrained minimization. Drori and Teboulle [2014] proposed to analyze the worst-case performance of a given first-order algorithm by numerically solving an additional optimization problem, which they called the Performance Estimation Problem (PEP). The authors formulated PEP as a nonconvex quadratic matrix program [Beck, 2007], which was then relaxed and solved via its dual SDP problem. Taylor et al. [2017b] later showed that the SDP reformulation is actually *exact* by introducing the notion of convex interpolation. To further improve the efficiency of solving PEP, researchers also developed various frameworks such as the Integral quadratic constraints (IQC) [Lessard et al., 2016] and

⁷https://pytorch.org/docs/stable/generated/torch.optim.lr_scheduler.ReduceLROnPlateau.html.

⁸A recent concurrent work [Bok and Altschuler, 2024] extends the silver stepsize schedule to projected GD. Note that projected GD is not a practical method for LP since the projections onto polyhedral constraints is as hard as solving the original LP [Lu, 2024].

nonconvex QCQP (especially for analyzing nonlinear conjugate gradient methods) [Gupta et al., 2023]. The development of PEP has led to many exciting advances in the theory of first-order methods, including tightening the classical bounds (e.g., [De Klerk et al., 2017, Fazlyab et al., 2018, De Klerk et al., 2020, Barré et al., 2020, Drori and Taylor, 2022, Teboulle and Vaisbourd, 2023] and all the works above), the construction of new Lyapunov functions [Taylor et al., 2018a, Taylor and Bach, 2019], performance estimation of a *given* monotone operator splitting method with constant “stepsize” [Ryu et al., 2020, Gu and Yang, 2020, Wang et al., 2019], and new analysis of ADMM [Nishihara et al., 2015, Seidman et al., 2019]. PEP can also be extended to tighten the complexity bound of projected or proximal gradient methods [Lessard et al., 2016, Taylor et al., 2017a, 2018b, Kim and Fessler, 2018a, d’Aspremont et al., 2021, Teboulle and Vaisbourd, 2023], mirror descent method [Dragomir et al., 2022], and very recently, Frank-Wolfe method [Luner and Grimmer, 2024]. It is worth mentioning that PEP requires a pre-determined T , so it falls into the finite horizon setup. **One key difference between these works and ours is that:** they focus on estimating the performance of a *given* algorithm, while we focus on designing new stepsize rules.

New algorithm design via PEP. In addition to analyzing a given algorithm, PEP also inspired many new algorithm designs. There are two mainstream approaches.

The first approach is to combine PEP with human expertise to inspire new proof ideas. This process often requires professional researchers to conduct SDP-based analysis, investigate the structure or the solution of PEP, and then manually generate a rigorous convergence proof. Following this approach, researchers have designed new stepsize design of GD [Grimmer et al., 2023, 2024a], new momentum mechanism [Kim and Fessler, 2016, Van Scoy et al., 2017, Cyrus et al., 2018, Yoon and Ryu, 2021, Taylor and Drori, 2023], new splitting method [Ryu and Vũ, 2020], and new method for composite nonsmooth saddle-point problem [Drori and Drori, 2014]. All these methods have asymptotic guarantees based on non-trivial design and proof. Their development requires human experts to conduct case-by-case exploration.

The second approach is to automatically search for a better design by introducing an “outer minimization problem” to PEP. While the PEP itself can be modeled as a convex problem (usually a SDP) [Drori and Teboulle, 2014, Taylor et al., 2017b], the overall minimax search problem is usually highly nonconvex [Drori and Teboulle, 2014, Das Gupta et al., 2024]. [Altschuler, 2018, Section 8] used algebraic techniques to solve the search problem analytically for $T \leq 3$. However, as commented by the authors, it seems difficult to extend these computations for a larger T . Drori and Teboulle [2014, Section 5] proposed to relax the nonconvex search problem to a convex SDP, and then they discovered an optimal stepsize rule for $T \leq 5$ (their Figure 4). Using similar convex relaxation or heuristics, researchers have discovered many new designs such as new momentum mechanism [Kim and Fessler, 2017, Drori, 2017, Drori and Taylor, 2020, Kim and Fessler, 2018b, 2021, Zhou et al., 2022, Park and Ryu, 2024], new proximal point methods [Kim, 2021, Lieder, 2021, Park and Ryu, 2022, Barré et al., 2023], and new cutting-plane methods [Drori and Teboulle, 2016]. Recently, Das Gupta et al. [2024] reformulated the overall minimax problem as a nonconvex QCQP proposed to solve it via customized spatial branch-and-bound algorithms. They then discovered the optimal stepsize schedule of GD up to $T = 25$. A similar stepsize schedule of GD for $T \leq 127$ are also discovered by “brute force searching” [Grimmer et al., 2023]. The methodologies in [Das Gupta et al., 2024] have also been extended to unconstrained nonsmooth problems to design new ISTA-type methods [Jang et al., 2023].

Our work is substantially different from the aforementioned works in three aspects. **First**, PEP framework is primarily designed for unconstrained minimization (and some closely related variants), while we focus on LP. It is widely recognized that linear programming (LP) exhibits many distinct structures and its algorithms are often developed in a tailored or specialized manner [Luenberger and Ye, 1984]. We study LP because: in engineering scenarios with strict time constraints (e.g., wireless communications, power systems, and autonomous vehicles), LP-related problems frequently emerge (see Section 1). This observation motivates us to re-design LP algorithms under a finite-horizon framework. **Second**, our stepsize design does not stem from PEP. Rather, it is an independently developed method. As a result, we have significantly different methodologies from PEP: PEP requires solving a *nonconvex* large-scale QCQP to design the optimal stepsize of GD, whereas we only require a *convex* small-scaled SDP with 4×4 matrices. The convexity of our search problem stems from LP. **Third**, PEP frameworks primarily focus on theoretical benefits, while we

focus on gaining speed-up on real-world LP benchmarks (in addition to theoretical guarantee).

Algorithms for LP. Since the 1940s, extensive research has been devoted to developing algorithms for LP. Today, the de-facto and mostly recognized methods include Dantzig’s simplex method [Dantzig, 2016, 1990] and interior-point methods (IPMs) [Karmarkar, 1984, Renegar, 1988, Monteiro and Adler, 1989, Nesterov and Nemirovskii, 1994, Wright, 1997, Ye, 2011]. Recently, first-order methods is becoming increasingly popular for solving large-scale LPs (e.g. [Chambolle and Pock, 2011, Goldstein et al., 2015, Applegate et al., 2021, Lin et al., 2021, Deng et al., 2022, Basu et al., 2020, O’Donoghue et al., 2016, O’Donoghue, 2021, Applegate et al., 2023, Lu and Yang, 2023a,b, Xiong and Freund, 2023, 2024, Xiong, 2024, Deng et al., 2024, Fercoq, 2024]). A more comprehensive review can be seen in [Lu, 2024]). Unlike simplex and IPMs, which require matrix factorization, first-order methods rely solely on matrix-vector multiplications. This makes them highly scalable on GPU and distributed computing platforms [Lu, 2024]. To our knowledge, we are the first work that re-design LP algorithms under the notion of “finite horizon”. We find that: if we abandon the asymptotic performance and instead focus on how the algorithm performs within a finite number of iterations, the primal-dual method can reach $3\times$ to $4\times$ acceleration by merely changing its stepsize design. We believe similar potential is inherently embedded in a wide range of LP algorithms, and our results might provide new perspectives to further accelerate the current methods.

7 Conclusion

In this work, we propose the framework of finite horizon optimization, which focus on algorithm design for the scenario where the total iteration budget is fixed and finite. We revisit the primal-dual method for LP and propose a new stepsize rule called Finite Horizon stepsize rule. We prove that this stepsize rule can reach an accelerated convergence rate at the T -th step, where T is the pre-determined total iteration budget. On a wide range of real-world LP instances, Finite Horizon stepsize rule reaches substantial speed-up over the optimal constant stepsize. One important future direction is to design Finite Horizon stepsize rules for more advanced algorithms, such as the momentum or the preconditioned variants of primal-dual method [Applegate et al., 2021]. It is also intriguing to apply the finite horizon framework to broader practical scenarios beyond LP.

Acknowledgement

The authors would like to thank Prof. Ruoyu Sun, Jiawei Zhang, Tian Ding, Prof. Tongxin Li, Wenzhi Gao, Xin Jiang, Ziniu Li, Xueyao Zhang, and group members of Prof. Mingyi Hong for the valuable discussions.

References

- J. Adler and O. Öktem. Learned primal-dual reconstruction. *IEEE transactions on medical imaging*, 37(6): 1322–1332, 2018.
- J. Altschuler. *Greed, hedging, and acceleration in convex optimization*. PhD thesis, Massachusetts Institute of Technology, 2018.
- J. M. Altschuler and P. A. Parrilo. Acceleration by stepsize hedging i: Multi-step descent and the silver stepsize schedule. *arXiv preprint arXiv:2309.07879*, 2023.
- J. M. Altschuler and P. A. Parrilo. Acceleration by stepsize hedging: Silver stepsize schedule for smooth convex optimization. *Mathematical Programming*, pages 1–14, 2024.

- D. Applegate, M. Díaz, O. Hinder, H. Lu, M. Lubin, B. O’Donoghue, and W. Schudy. Practical large-scale linear programming using primal-dual hybrid gradient. *Advances in Neural Information Processing Systems*, 34:20243–20257, 2021.
- D. Applegate, O. Hinder, H. Lu, and M. Lubin. Faster first-order primal-dual methods for linear programming using restarts and sharpness. *Mathematical Programming*, 201(1):133–184, 2023.
- S. Babaeinejadsarookolae, A. Birchfield, R. D. Christie, C. Coffrin, C. DeMarco, R. Diao, M. Ferris, S. Fliscounakis, S. Greene, R. Huang, et al. The power grid library for benchmarking ac optimal power flow algorithms. *arXiv preprint arXiv:1908.02788*, 2019.
- M. Barré, A. Taylor, and A. d’Aspremont. Complexity guarantees for polyak steps with momentum. In *Conference on learning theory*, pages 452–478. PMLR, 2020.
- M. Barré, A. B. Taylor, and F. Bach. Principled analyses and design of first-order methods with inexact proximal operators. *Mathematical Programming*, 201(1):185–230, 2023.
- J. Barzilai and J. M. Borwein. Two-point step size gradient methods. *IMA journal of numerical analysis*, 8(1): 141–148, 1988.
- K. Basu, A. Ghoting, R. Mazumder, and Y. Pan. Eclipse: An extreme-scale linear program solver for web-applications. In *International Conference on Machine Learning*, pages 704–714. PMLR, 2020.
- A. Beck. Quadratic matrix programming. *SIAM Journal on Optimization*, 17(4):1224–1238, 2007.
- L. Boher, R. Rabineau, and M. Helard. Fpga implementation of an iterative receiver for mimo-ofdm systems. *IEEE Journal on Selected Areas in Communications*, 26(6):857–866, 2008.
- J. Bok and J. M. Altschuler. Accelerating proximal gradient descent via silver stepsizes. *arXiv preprint arXiv:2412.05497*, 2024.
- S. Boyd and L. Vandenberghe. *Convex optimization*. Cambridge university press, 2004.
- Y. Cai, J. Wu, S. Mei, M. Lindsey, and P. L. Bartlett. Large stepsize gradient descent for non-homogeneous two-layer networks: Margin improvement and fast optimization. *arXiv preprint arXiv:2406.08654*, 2024.
- A. Cauchy et al. Méthode générale pour la résolution des systemes d’équations simultanées. *Comp. Rend. Sci. Paris*, 25(1847):536–538, 1847.
- A. Chambolle and T. Pock. A first-order primal-dual algorithm for convex problems with applications to imaging. *Journal of mathematical imaging and vision*, 40:120–145, 2011.
- G. C. Chasparis and J. S. Shamma. Linear-programming-based multi-vehicle path planning with adversaries. In *Proceedings of the 2005, American Control Conference, 2005.*, pages 1072–1077. IEEE, 2005.
- S. Chatzivasileiadis. Optimal power flow (dc-opf and ac-opf). *DTU Summer School*, 2018.
- P. L. Chebyshev. *Théorie des mécanismes connus sous le nom de parallélogrammes*. Imprimerie de l’Académie impériale des sciences, 1853.
- T. Chen, X. Chen, W. Chen, H. Heaton, J. Liu, Z. Wang, and W. Yin. Learning to optimize: A primer and a benchmark. *Journal of Machine Learning Research*, 23(189):1–59, 2022.
- Y. Chen, J. Han, and X. Zhao. Three-dimensional path planning for unmanned aerial vehicle based on linear programming. *Robotica*, 30(5):773–781, 2012.
- R. D. Christie, B. F. Wollenberg, and I. Wangensteen. Transmission management in the deregulated environment. *Proceedings of the IEEE*, 88(2):170–195, 2000.

- K. F. Culligan. *Online trajectory planning for UAVs using mixed integer linear programming*. PhD thesis, Massachusetts Institute of Technology, 2006.
- S. Cyrus, B. Hu, B. Van Scoy, and L. Lessard. A robust accelerated optimization algorithm for strongly convex functions. In *2018 Annual American Control Conference (ACC)*, pages 1376–1381. IEEE, 2018.
- A. Daccache, F. Glineur, and J. Hendrickx. *Performance estimation of the gradient method with fixed arbitrary step sizes*. PhD thesis, Master’s thesis, Université Catholique de Louvain, 2019.
- G. B. Dantzig. Origins of the simplex method. In *A history of scientific computing*, pages 141–151. 1990.
- G. B. Dantzig. Linear programming. *Operations research*, 50(1):42–47, 2002.
- G. B. Dantzig. Linear programming and extensions. In *Linear programming and extensions*. Princeton university press, 2016.
- S. Das Gupta, B. P. Van Parys, and E. K. Ryu. Branch-and-bound performance estimation programming: A unified methodology for constructing optimal optimization methods. *Mathematical Programming*, 204(1): 567–639, 2024.
- E. De Klerk, F. Glineur, and A. B. Taylor. On the worst-case complexity of the gradient method with exact line search for smooth strongly convex functions. *Optimization Letters*, 11:1185–1199, 2017.
- E. De Klerk, F. Glineur, and A. B. Taylor. Worst-case convergence analysis of inexact gradient and newton methods through semidefinite programming performance estimation. *SIAM Journal on Optimization*, 30(3): 2053–2082, 2020.
- A. Defazio, A. Cutkosky, H. Mehta, and K. Mishchenko. When, why and how much? adaptive learning rate scheduling by refinement. *arXiv preprint arXiv:2310.07831*, 2023.
- A. Defazio, X. A. Yang, H. Mehta, K. Mishchenko, A. Khaled, and A. Cutkosky. The road less scheduled. *arXiv preprint arXiv:2405.15682*, 2024.
- Q. Deng, Q. Feng, W. Gao, D. Ge, B. Jiang, Y. Jiang, J. Liu, T. Liu, C. Xue, Y. Ye, et al. New developments of admm-based interior point methods for linear programming and conic programming. *arXiv preprint arXiv:2209.01793*, 2022.
- Q. Deng, Q. Feng, W. Gao, D. Ge, B. Jiang, Y. Jiang, J. Liu, T. Liu, C. Xue, Y. Ye, et al. An enhanced alternating direction method of multipliers-based interior point method for linear and conic optimization. *INFORMS Journal on Computing*, 2024.
- D. Dolgov, S. Thrun, M. Montemerlo, and J. Diebel. Practical search techniques in path planning for autonomous driving. *Ann Arbor*, 1001(48105):18–80, 2008.
- R.-A. Dragomir, A. B. Taylor, A. d’Aspremont, and J. Bolte. Optimal complexity and certification of bregman first-order methods. *Mathematical Programming*, pages 1–43, 2022.
- Y. Drori. The exact information-based complexity of smooth convex minimization. *Journal of Complexity*, 39: 1–16, 2017.
- Y. Drori and Y. Drori. *Contributions to the complexity analysis of optimization algorithms*. Universitat Tel-Aviv Tel Aviv, Israel, 2014.
- Y. Drori and A. Taylor. On the oracle complexity of smooth strongly convex minimization. *Journal of Complexity*, 68:101590, 2022.
- Y. Drori and A. B. Taylor. Efficient first-order methods for convex minimization: a constructive approach. *Mathematical Programming*, 184(1):183–220, 2020.

- Y. Drori and M. Teboulle. Performance of first-order methods for smooth convex minimization: a novel approach. *Mathematical Programming*, 145(1):451–482, 2014.
- Y. Drori and M. Teboulle. An optimal variant of Kelley’s cutting-plane method. *Mathematical Programming*, 160:321–351, 2016.
- A. d’Aspremont, D. Scieur, A. Taylor, et al. Acceleration methods. *Foundations and Trends® in Optimization*, 5(1-2):1–245, 2021.
- D. Eloi and F. Glineur. *Worst-case functions for the gradient method with fixed variable step sizes*. PhD thesis, Master’s thesis, Université Catholique de Louvain, 2022.
- M. Fazlyab, A. Ribeiro, M. Morari, and V. M. Preciado. Analysis of optimization algorithms via integral quadratic constraints: Nonstrongly convex problems. *SIAM Journal on Optimization*, 28(3):2654–2689, 2018.
- O. Fercoq. Monitoring the convergence speed of pdhg to find better primal and dual step sizes. *arXiv preprint arXiv:2403.19202*, 2024.
- O. Ferraz, S. Subramaniyan, R. Chinthala, J. Andrade, J. R. Cavallaro, S. K. Nandy, V. Silva, X. Zhang, M. Purnaprajna, and G. Falcao. A survey on high-throughput non-binary ldpc decoders: Asic, fpga, and gpu architectures. *IEEE Communications Surveys & Tutorials*, 24(1):524–556, 2021.
- S. Frank, I. Steponavice, and S. Rebennack. Optimal power flow: A bibliographic survey i: Formulations and deterministic methods. *Energy systems*, 3:221–258, 2012.
- H. Fu, C. Li, X. Liu, J. Gao, A. Celikyilmaz, and L. Carin. Cyclical annealing schedule: A simple approach to mitigating kl vanishing. *arXiv preprint arXiv:1903.10145*, 2019.
- D. M. Gay. Electronic mail distribution of linear programming test problems. *Mathematical Programming Society COAL Newsletter*, 13:10–12, 1985.
- T. Goldstein, M. Li, and X. Yuan. Adaptive primal-dual splitting methods for statistical learning and image processing. *Advances in neural information processing systems*, 28, 2015.
- B. Goujaud, D. Scieur, A. Dieuleveut, A. B. Taylor, and F. Pedregosa. Super-acceleration with cyclical step-sizes. In *International Conference on Artificial Intelligence and Statistics*, pages 3028–3065. PMLR, 2022.
- P. Goyal, P. Dollár, R. Girshick, P. Noordhuis, L. Wesolowski, A. Kyrola, A. Tulloch, Y. Jia, and K. He. Accurate, large minibatch sgd: Training imagenet in 1 hour. arxiv 2017. *arXiv preprint arXiv:1706.02677*, 2017.
- K. Gregor and Y. LeCun. Learning fast approximations of sparse coding. In *Proceedings of the 27th international conference on international conference on machine learning*, pages 399–406, 2010.
- B. Grimmer. Provably faster gradient descent via long steps. *SIAM Journal on Optimization*, 34(3):2588–2608, 2024.
- B. Grimmer, K. Shu, and A. L. Wang. Accelerated gradient descent via long steps. *arXiv preprint arXiv:2309.09961*, 2023.
- B. Grimmer, K. Shu, and A. L. Wang. Accelerated objective gap and gradient norm convergence for gradient descent via long steps. *arXiv preprint arXiv:2403.14045*, 2024a.
- B. Grimmer, K. Shu, and A. L. Wang. Composing optimized stepsize schedules for gradient descent. *arXiv preprint arXiv:2410.16249*, 2024b.
- B. Grimmer, K. Shu, and A. L. Wang. A strengthened conjecture on the minimax optimal constant stepsize for gradient descent. *arXiv preprint arXiv:2407.11739*, 2024c.

- G. Gu and J. Yang. Tight sublinear convergence rate of the proximal point algorithm for maximal monotone inclusion problems. *SIAM Journal on Optimization*, 30(3):1905–1921, 2020.
- S. D. Gupta, R. M. Freund, X. A. Sun, and A. Taylor. Nonlinear conjugate gradient methods: worst-case convergence rates via computer-assisted analyses. *arXiv preprint arXiv:2301.01530*, 2023.
- K. He, X. Zhang, S. Ren, and J. Sun. Deep residual learning for image recognition. In *Proceedings of the IEEE conference on computer vision and pattern recognition*, pages 770–778, 2016.
- R. A. Horn and C. R. Johnson. *Matrix analysis*. Cambridge university press, 2012.
- S. Hu, Y. Tu, X. Han, C. He, G. Cui, X. Long, Z. Zheng, Y. Fang, Y. Huang, W. Zhao, et al. Minicpm: Unveiling the potential of small language models with scalable training strategies. *arXiv preprint arXiv:2404.06395*, 2024.
- A. Ibrahim, B. Thérien, K. Gupta, M. L. Richter, Q. Anthony, T. Lesort, E. Belilovsky, and I. Rish. Simple and scalable strategies to continually pre-train large language models. *arXiv preprint arXiv:2403.08763*, 2024.
- U. Jang, S. D. Gupta, and E. K. Ryu. Computer-assisted design of accelerated composite optimization methods: Optista. *arXiv preprint arXiv:2305.15704*, 2023.
- L. V. Kantorovich. Mathematical methods of organizing and planning production. *Management science*, 6(4): 366–422, 1960.
- N. Karmarkar. A new polynomial-time algorithm for linear programming. In *Proceedings of the sixteenth annual ACM symposium on Theory of computing*, pages 302–311, 1984.
- J. Kelner, A. Marsden, V. Sharan, A. Sidford, G. Valiant, and H. Yuan. Big-step-little-step: Efficient gradient methods for objectives with multiple scales. In *Conference on Learning Theory*, pages 2431–2540. PMLR, 2022.
- D. Kiessling, A. Zanelli, A. Nurkanović, J. Gillis, M. Diehl, M. Zeilinger, G. Pipeleers, and J. Swevers. A feasible sequential linear programming algorithm with application to time-optimal path planning problems. In *2022 IEEE 61st Conference on Decision and Control (CDC)*, pages 1196–1203. IEEE, 2022.
- D. Kim. Accelerated proximal point method for maximally monotone operators. *Mathematical Programming*, 190(1):57–87, 2021.
- D. Kim and J. A. Fessler. Optimized first-order methods for smooth convex minimization. *Mathematical programming*, 159:81–107, 2016.
- D. Kim and J. A. Fessler. On the convergence analysis of the optimized gradient method. *Journal of optimization theory and applications*, 172(1):187–205, 2017.
- D. Kim and J. A. Fessler. Another look at the fast iterative shrinkage/thresholding algorithm (fista). *SIAM Journal on Optimization*, 28(1):223–250, 2018a.
- D. Kim and J. A. Fessler. Generalizing the optimized gradient method for smooth convex minimization. *SIAM Journal on Optimization*, 28(2):1920–1950, 2018b.
- D. Kim and J. A. Fessler. Optimizing the efficiency of first-order methods for decreasing the gradient of smooth convex functions. *Journal of optimization theory and applications*, 188(1):192–219, 2021.
- F. Kittaneh. Spectral radius inequalities for hilbert space operators. *Proceedings of the American Mathematical Society*, pages 385–390, 2006.
- G. Kornowski and O. Shamir. Open problem: Anytime convergence rate of gradient descent. *arXiv preprint arXiv:2406.13888*, 2024.

- M. Latva-Aho, K. Leppänen, et al. Key drivers and research challenges for 6g ubiquitous wireless intelligence. 2019.
- L. Lessard, B. Recht, and A. Packard. Analysis and design of optimization algorithms via integral quadratic constraints. *SIAM Journal on Optimization*, 26(1):57–95, 2016.
- B. Li, L. Yang, Y. Chen, S. Wang, Q. Chen, H. Mao, Y. Ma, A. Wang, T. Ding, J. Tang, et al. Pdhg-unrolled learning-to-optimize method for large-scale linear programming. *arXiv preprint arXiv:2406.01908*, 2024.
- D. Li and R. Sun. On a faster r -linear convergence rate of the barzilai-borwein method. *arXiv preprint arXiv:2101.00205*, 2021.
- G. Li, X. Zhang, H. Guo, B. Lenzo, and N. Guo. Real-time optimal trajectory planning for autonomous driving with collision avoidance using convex optimization. *Automotive Innovation*, 6(3):481–491, 2023.
- F. Lieder. On the convergence rate of the halpern-iteration. *Optimization letters*, 15(2):405–418, 2021.
- T. Lin, S. Ma, Y. Ye, and S. Zhang. An admm-based interior-point method for large-scale linear programming. *Optimization Methods and Software*, 36(2-3):389–424, 2021.
- I. Loshchilov and F. Hutter. Sgdr: Stochastic gradient descent with warm restarts. *arXiv preprint arXiv:1608.03983*, 2016.
- H. Lu. First-order methods for linear programming. *arXiv preprint arXiv:2403.14535*, 2024.
- H. Lu and J. Yang. cupdlp.jl: A gpu implementation of restarted primal-dual hybrid gradient for linear programming in julia. *arXiv preprint arXiv:2311.12180*, 2023a.
- H. Lu and J. Yang. On a unified and simplified proof for the ergodic convergence rates of ppm, pdhg and admm. *arXiv preprint arXiv:2305.02165*, 2023b.
- D. G. Luenberger and Y. Ye. *Linear and nonlinear programming*, volume 2. Springer, 1984.
- A. Luner and B. Grimmer. Performance estimation for smooth and strongly convex sets. *arXiv preprint arXiv:2410.14811*, 2024.
- W. Markov and J. Grossmann. Über polynome, die in einem gegebenen intervall möglichst wenig von null abweichen. *Mathematische Annalen*, 77(2):213–258, 1916.
- L. Mones. A gentle introduction to optimal power flow. <https://invenia.github.io/blog/2021/06/18/opf-intro/>, 2021.
- V. Monga, Y. Li, and Y. C. Eldar. Algorithm unrolling: Interpretable, efficient deep learning for signal and image processing. *IEEE Signal Processing Magazine*, 38(2):18–44, 2021.
- R. D. Monteiro and I. Adler. Interior path following primal-dual algorithms. part i: Linear programming. *Mathematical programming*, 44(1):27–41, 1989.
- Y. Nesterov. A method for solving the convex programming problem with convergence rate $o(1/k^2)$. In *Dokl akad nauk Sssr*, volume 269, page 543, 1983.
- Y. Nesterov and A. Nemirovskii. *Interior-point polynomial algorithms in convex programming*. SIAM, 1994.
- Y. Nesterov et al. *Lectures on convex optimization*, volume 137. Springer, 2018.
- R. Nishihara, L. Lessard, B. Recht, A. Packard, and M. Jordan. A general analysis of the convergence of admm. In *International conference on machine learning*, pages 343–352. PMLR, 2015.

- B. O’Donoghue. Operator splitting for a homogeneous embedding of the linear complementarity problem. *SIAM Journal on Optimization*, 31(3):1999–2023, 2021.
- S. Oymak. Provable super-convergence with a large cyclical learning rate. *IEEE Signal Processing Letters*, 28:1645–1649, 2021.
- B. O’Donoghue, E. Chu, N. Parikh, and S. Boyd. Conic optimization via operator splitting and homogeneous self-dual embedding. *Journal of Optimization Theory and Applications*, 169:1042–1068, 2016.
- X. Pan. Deepopf: deep neural networks for optimal power flow. In *Proceedings of the 8th ACM International Conference on Systems for Energy-Efficient Buildings, Cities, and Transportation*, pages 250–251, 2021.
- C. Park and E. K. Ryu. Optimal first-order algorithms as a function of inequalities. *Journal of Machine Learning Research*, 25, 2024.
- J. Park and E. K. Ryu. Exact optimal accelerated complexity for fixed-point iterations. In *International Conference on Machine Learning*, pages 17420–17457. PMLR, 2022.
- P. Pedregal. *Introduction to optimization*, volume 46. Springer, 2004.
- F. Pedregosa. Residual polynomials and the chebyshev method. <http://fa.bianp.net/blog/2020/polyopt/>, 2020.
- B. T. Polyak. Some methods of speeding up the convergence of iteration methods. *Ussr computational mathematics and mathematical physics*, 4(5):1–17, 1964.
- X. Qian, F. Altché, P. Bender, C. Stiller, and A. de La Fortelle. Optimal trajectory planning for autonomous driving integrating logical constraints: An miqp perspective. In *2016 IEEE 19th international conference on intelligent transportation systems (ITSC)*, pages 205–210. IEEE, 2016.
- J. Renegar. A polynomial-time algorithm, based on newton’s method, for linear programming. *Mathematical programming*, 40(1):59–93, 1988.
- T. Rotaru, F. Glineur, and P. Patrinos. Exact worst-case convergence rates of gradient descent: a complete analysis for all constant stepsizes over nonconvex and convex functions. *arXiv preprint arXiv:2406.17506*, 2024.
- E. K. Ryu and B. C. Vũ. Finding the forward-douglas–rachford-forward method. *Journal of Optimization Theory and Applications*, 184(3):858–876, 2020.
- E. K. Ryu, A. B. Taylor, C. Bergeling, and P. Giselsson. Operator splitting performance estimation: Tight contraction factors and optimal parameter selection. *SIAM Journal on Optimization*, 30(3):2251–2271, 2020.
- Y. Saad. *Iterative methods for sparse linear systems*. SIAM, 2003.
- A. Schrijver. *Theory of linear and integer programming*. John Wiley & Sons, 1998.
- J. H. Seidman, M. Fazlyab, V. M. Preciado, and G. J. Pappas. A control-theoretic approach to analysis and parameter selection of douglas–rachford splitting. *IEEE Control Systems Letters*, 4(1):199–204, 2019.
- Q. Shi, M. Razaviyayn, Z.-Q. Luo, and C. He. An iteratively weighted mmse approach to distributed sum-utility maximization for a mimo interfering broadcast channel. *IEEE Transactions on Signal Processing*, 59(9):4331–4340, 2011.
- L. N. Smith. Cyclical learning rates for training neural networks. In *2017 IEEE winter conference on applications of computer vision (WACV)*, pages 464–472. IEEE, 2017.
- J. K. Subitsits and J. C. Gerdes. From the racetrack to the road: Real-time trajectory replanning for autonomous driving. *IEEE Transactions on Intelligent Vehicles*, 4(2):309–320, 2019.

- H. Sun, X. Chen, Q. Shi, M. Hong, X. Fu, and N. D. Sidiropoulos. Learning to optimize: Training deep neural networks for interference management. *IEEE Transactions on Signal Processing*, 66(20):5438–5453, 2018.
- J. Sun, H. Li, Z. Xu, et al. Deep admm-net for compressive sensing mri. *Advances in neural information processing systems*, 29, 2016.
- R. Sun and Y. Ye. Worst-case complexity of cyclic coordinate descent: $O(n^2)$ gap with randomized version. *Mathematical Programming*, 185:487–520, 2021.
- R. Sun, Z.-Q. Luo, and Y. Ye. On the efficiency of random permutation for admm and coordinate descent. *Mathematics of Operations Research*, 45(1):233–271, 2020.
- R.-Y. Sun. Optimization for deep learning: An overview. *Journal of the Operations Research Society of China*, 8(2):249–294, 2020.
- M. Sy. Optimization strategies for low-latency 5g nr ldpc decoding on general purpose processor. In *2023 International Conference on Control, Communication and Computing (ICCC)*, pages 1–6. IEEE, 2023.
- Y. Tang, K. Dvijotham, and S. Low. Real-time optimal power flow. *IEEE Transactions on Smart Grid*, 8(6):2963–2973, 2017.
- A. Taylor and F. Bach. Stochastic first-order methods: non-asymptotic and computer-aided analyses via potential functions. In *Conference on Learning Theory*, pages 2934–2992. PMLR, 2019.
- A. Taylor and Y. Drori. An optimal gradient method for smooth strongly convex minimization. *Mathematical Programming*, 199(1):557–594, 2023.
- A. Taylor, B. Van Scoy, and L. Lessard. Lyapunov functions for first-order methods: Tight automated convergence guarantees. In *International Conference on Machine Learning*, pages 4897–4906. PMLR, 2018a.
- A. B. Taylor, J. M. Hendrickx, and F. Glineur. Exact worst-case performance of first-order methods for composite convex optimization. *SIAM Journal on Optimization*, 27(3):1283–1313, 2017a.
- A. B. Taylor, J. M. Hendrickx, and F. Glineur. Smooth strongly convex interpolation and exact worst-case performance of first-order methods. *Mathematical Programming*, 161:307–345, 2017b.
- A. B. Taylor, J. M. Hendrickx, and F. Glineur. Exact worst-case convergence rates of the proximal gradient method for composite convex minimization. *Journal of Optimization Theory and Applications*, 178:455–476, 2018b.
- M. Teboulle and Y. Vaisbourd. An elementary approach to tight worst case complexity analysis of gradient based methods. *Mathematical Programming*, 201(1):63–96, 2023.
- O. Toupet. *Real-time path-planning using mixed-integer linear programming and global cost-to-go maps*. PhD thesis, Massachusetts Institute of Technology, 2006.
- C. Tsallis. Possible generalization of boltzmann-gibbs statistics. *Journal of statistical physics*, 52:479–487, 1988.
- B. Van Scoy, R. A. Freeman, and K. M. Lynch. The fastest known globally convergent first-order method for minimizing strongly convex functions. *IEEE Control Systems Letters*, 2(1):49–54, 2017.
- B. Wang, S. Ma, J. Yang, and D. Zhou. Relaxed proximal point algorithm: Tight complexity bounds and acceleration without momentum. *arXiv preprint arXiv:2410.08890*, 2024.
- H. Wang, M. Fazlyab, S. Chen, and V. M. Preciado. Robust convergence analysis of three-operator splitting. In *2019 57th Annual Allerton Conference on Communication, Control, and Computing (Allerton)*, pages 391–398. IEEE, 2019.

- K. Wen, Z. Li, J. Wang, D. Hall, P. Liang, and T. Ma. Understanding warmup-stable-decay learning rates: A river valley loss landscape perspective. *arXiv preprint arXiv:2410.05192*, 2024.
- S. J. Wright. *Primal-dual interior-point methods*. SIAM, 1997.
- J. Wu, P. L. Bartlett, M. Telgarsky, and B. Yu. Large stepsize gradient descent for logistic loss: Non-monotonicity of the loss improves optimization efficiency. *arXiv preprint arXiv:2402.15926*, 2024.
- Y. Xiang, S. Gubian, B. Suomela, and J. Hoeng. Generalized simulated annealing for global optimization: the gensa package. *R J.*, 5(1):13, 2013.
- Z. Xiong. Accessible theoretical complexity of the restarted primal-dual hybrid gradient method for linear programs with unique optima. *arXiv preprint arXiv:2410.04043*, 2024.
- Z. Xiong and R. M. Freund. Computational guarantees for restarted pdhg for lp based on" limiting error ratios" and lp sharpness. *arXiv preprint arXiv:2312.14774*, 2023.
- Z. Xiong and R. M. Freund. The role of level-set geometry on the performance of pdhg for conic linear optimization. *arXiv preprint arXiv:2406.01942*, 2024.
- Y. Yang, J. Sun, H. Li, and Z. Xu. Admm-csnet: A deep learning approach for image compressive sensing. *IEEE transactions on pattern analysis and machine intelligence*, 42(3):521–538, 2018.
- Y. Ye. *Interior point algorithms: theory and analysis*. John Wiley & Sons, 2011.
- T. Yoon and E. K. Ryu. Accelerated algorithms for smooth convex-concave minimax problems with $o(1/k^2)$ rate on squared gradient norm. In *International Conference on Machine Learning*, pages 12098–12109. PMLR, 2021.
- D. Young. On richardson's method for solving linear systems with positive definite matrices. *Journal of Mathematics and Physics*, 32(1-4):243–255, 1953.
- D. M. Young. *Iterative solution of large linear systems*. Elsevier, 2014.
- M. Yu and C. Fan. Rigid body path planning using mixed-integer linear programming. *IEEE Robotics and Automation Letters*, 2024.
- L. Zhang, Y. Chen, and B. Zhang. A convex neural network solver for dcof with generalization guarantees. *IEEE Transactions on Control of Network Systems*, 9(2):719–730, 2021.
- Z. Zhang and R. Jiang. Accelerated gradient descent by concatenation of stepsize schedules. *arXiv preprint arXiv:2410.12395*, 2024.
- Z. Zhang, J. D. Lee, S. S. Du, and Y. Chen. Anytime acceleration of gradient descent. *arXiv preprint arXiv:2411.17668*, 2024.
- K. Zhou, L. Tian, A. M.-C. So, and J. Cheng. Practical schemes for finding near-stationary points of convex finite-sums. In *International Conference on Artificial Intelligence and Statistics*, pages 3684–3708. PMLR, 2022.

A More Results

More results related to Figure 1 (b). Figure 1 (b) presents the curves of optimality gap and the detailed stepsize rules. We find that the optimal constant stepsize cannot reach optimal solutions until > 200 steps, while the Finite Horizon stepsize rule solves the problem in 2 steps. The experimental setup is the same as in Section 5.1 except that we change the initialization to $N(80, 1)$ for better visualization.

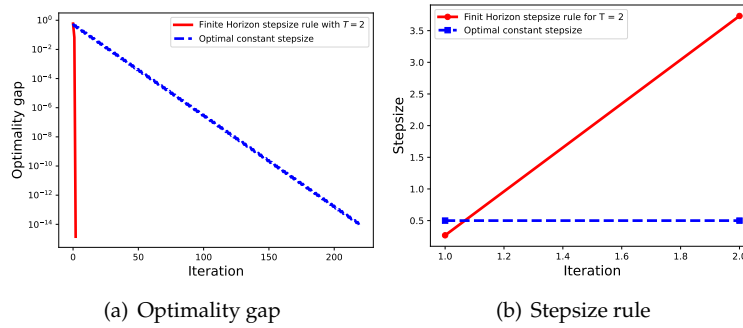


Figure 8: The curves of optimality gap and the detailed stepsize rules (for the first 2 steps) of the results in Figure 1.